ON TURBULENT FLOW BETWEEN ROTATING CYLINDERS

Thesis by

Pai Shih - I

In Partial Fulfillment of the Requirements for the Degree of

Doctor of Philosophy

California Institute of Technology

Pasadena, California

1939

Acknowledgement

The author wishes to express his sincere appreciation for the inspiration and guidance of Dr. von Karman during these investigations, to Dr. C.B. Millikan for his kind interest and advice, to Mr. Carl Thiele for help and suggestions regarding apparatus, and to all others of the Guggenheim staff.

Table of Contents

On Turbulent Flow Between Rotating Cylinders

Abstract.

The present work had as its purpose the investigation of the velocity and turbulence distributions in the turbulent flow between two co-axial cylinders, the inner of which rotated. The radius of the inner cylinder was 7-7/8". Two aspect ratios were used, one 10" to 1-1/16", the other 10" to 17/32". All velocity and turbulence measurements were made with hot-wire technique, using a special holder which reduced spindle interference to a minimum.

The circumferential velocity of the inner rotating cylinder was several hundred times the critical speed for instability of the laminar flow as given by G.I.Taylor.

It was found that velocity distributions in which the circumferential velocity of the fluid increases outward actually exist and cannot be explained by the shadow effect of the measuring instrument as G.I.Taylor suggested. Also the flow between the rotating cylinders is three-dimensional. The mean velocity distribution depends on whether the transfer of shear is carried out by turbulent fluctuations or by secondary motion. The regions, where the secondary motion is negligible, the mean velocity distribution is logarithmic which was shown by Dr. von Karman to be the distribution in Couette's case of turbulent flow.

The analysis of the measurements indicated that the secondary flow can be described by assuming ring-shaped vor-

tices between the cylinders. It was known that such ring-shaped vortices introduce the instability of the laminar flow (see Ref.1); but it was not known that such vortices exist at speeds as high as several hundred times the critical speed for instability, although their shapes are distorted. The sizes of the vortices and their numbers depend on the speed of the inner cylinder. The vortices can only exist in pairs, and at certain critical speeds the flow pattern may change suddenly due to the loss or gain of a pair of vortices. At high speeds the number of the vortices tends to decrease.

The two-dimensional theories for turbulent flow between rotating cylinders are discussed. They can not even be taken as a first approximation for this three dimensional vortex-ring flow.

List of Figures

Introduction.

The flow between co-axial rotating cylinders is known as Couette's type of curved flow. The exact mean velocity distribution for turbulent flow in this case is not yet known. It was the purpose of this research to investigate experimentally the velocity and turbulence distributions for the turbulent flow between two coaxial cylinders.

G.I.Taylor has investigated this flow with the inner cylinder rotating and outer one at rest. He measured the total pressure distribution across the gap, and assumed a shadow effect of the measuring instrument; i.e. the difference between the measured pressure with a pitot tube of finite bore and that which would be measured if the pitot tube did not obstruct the flow is proportional to the resistance of the pitot tube. By such an extrapolation of the results, Taylor found that the experimental results satisfied his vorticity transport theory. However the validity of such extrapolation is somewhat in doubt.

In the present work, a special measuring device was designed, which, we have assumed, reduced this shadow effect to a negligible amount.

To make sure that the flow investigated was turbulent the inner cylinder was rotated and the outer one held stationary, since this is the most unstable case. The operating speeds were several hundred times that critical speed necessary for turbulence as given by G.I.Taylor.

The measurements of turbulence and mean velocity were carried out by the use of a hot-wire anemometer.

Description of Apparatus.

1. Cylinders.

The apparatus consisted of two cylinders mounted on a rigid frame made of steel angle stock as shown in Fig.1. The inner cylinder was cast of an alluminum alloy, turned true to ±0.002", and carefully balanced to eliminate vibration. Its outer diameter was 15-3/4" and its length 11". The cylinder was ordinarily turned by a 1/10 hp. synchronous motor coupled rigidly to its shaft. A belt drive to a 1/4 hp. d.c. motor was also provided, but it was used only when the variable frequency source was not available.

The inside of the inner cylinder was sealed by wooden plates and wax so that the possibility of circulation from the gap to the inside of the inner cylinder was eliminated.

Two similar outer cylinders with different diameters were used. They were turned of wood and had 1" walls. Their inner diameters were 16-13/16" and 17-7/8" and hence the gaps were 17/32" and 1-1/16" respectively.

It was desirable that both ends have identical seals. Hence at the bottom of the outer cylinder, a series of 3/4" holes were drilled around its circumference. Two wooden rings with a width just a little less than the gap between the cylinders were attached to the outer cylinder. One ring was at the top edge of the outer cylinder and the other was just above the bottom holes. The clearance between the wooden ring and the inner cylinder was sealed by felt. Thus both ends

were nearly at atmospheric pressure.

The hot-wire was inserted at the central part of the outer cylinder. The schematical diagram of the holder is shown in Fig.2. The hot-wire was soldered across the 1/2" gap shown in the figure. Since the spindles were far from the hot-wire, the effect of their wake was negligible. The spindles were mounted on a block which rested on a slide so that the spindles could travel back and forth with the block as a whole. The slide was moved by a micrometer which indicated the position of the hot-wire in the space between the cylinders.

The front part of the hot-wire holder which was inserted into the outer cylinder, was made of hard rubber. In order to obtain a good fit between the hot-wire holder and the cylinder, a brass slot was made and set into the wall of the outer cylinder. The inside of the outer cylinder, the brass slot and the hard rubber holder were turned as one piece and painted simultaneously. Therefore these three pieces formed a smooth cylindrical surface.

A series of static holes, fifteen in number, was drilled along an element of the outer cylinder. These static holes gave an indication of the flow pattern in the gap.

The r.p.m. of the inner cylinder was measured by means of a ten pole generator attached to the shaft of the

drive motor. The output of this generator was compared with that of a calibrated oscillator by the Lessajou figures formed on a cathode ray oscilloscope.

2. Hot-Wire Anemometer.

The hot-wire anemometer used was the No.2 Galcit hot-wire anemometer which consisted of three main parts, namely: 1. hot-wire and its heating circuit, 2. vacuum tube amplifier, and 3, output instruments.

Two types of hot wires were used: 0.001" diameter pure platinum wire for mean speed and 0.0005" diameter Wollaston wire for turbulence. The diagram of the heating circuit is shown in Fig.3, which is essentially the conventional Wheat-stone bridge circuit.

In turbulence measurement, the fluctuating voltage drop produced by speed fluctuations acting on the hot-wrie is usually of the order of a few thousandths of a volt and therefore must be amplified. The circuit of the vacuum tube amplifier used is shown in Fig.4. The amplifier is a four-stage high gain resistance-capacity coupled amplifier, compensated for the lag of the hot-wire. The response of the amplifier, uncompensated and compensated, is shown in Figs. 5 and 6, respectively. The output of the amplifier was measured by a thermocouple used in conjunction with a wall galvanometer.

In addition, the output could be measured by an a.c. voltmeter, which was used to indicate its approximate magnitude; or by cathode ray oscilloscope, which was used for visual inspection of the wave form. A complete description of this hot-wire anemometer is given in reference 12.

Description of Measurements.

Traverse were carried out at several different rotating speeds of the inner cylinder and at seveal axial positions for each aspect ratio. During each traverse, the distribution of the static pressure was recorded.

The hot wires used were calibrated in a small tunnel. When used for turbulence, the ordinary calculations were applied. Since the holder was very large, the Galcit vibrator (see refernce 12) could not be used to calibrate the wires. However a wire similar to those used was so calibrated and its lag constant, M (see refernce 7), was found to agree well with the computed value.

Turbulence Criterion.

The instability of an ideal fluid in circulatory motion was first investigated by Lord Reyleigh. He considered the equilibrium conditions between the pressure gradient along a radius r and the centrifugal force. He found that the stability of the velocity distribution depends upon the variation of the product Uxr, where U is the linear circumferential velocity and r the distance from the center. If the product Uxr increases with increasing radius the velocity distribution is stable, while in the opposite case it is unstable.

G.I.Taylor extended Rayleigh's investigation to the case of viscous fluid in laminar motion, e.g., to the case of laminar circulatory motion between two rotating cylinders. According to Taylor's results the range of stability is enlarged. On the assumption of symmetrical disturbance the criterion for stability of a viscous fluid in steady motion between concentric rotating cylinders was found. The exact criterion is too complicated to be used. However an approximate form for the criterion was developed which is useful for numerical computation. We are going to apply this approximate criterion for our two cases as follows:

When the gap is small in comparison with both radii of the rotating cylinders and when the ratio of the rotating speeds of the two cylinders w lies between 0 and 1, the

approximate criterion may be stated as below:

$$P = 0.0571\left(\frac{1+w}{1-w} - 0.652\,\frac{d}{R_1}\right)+0.00056\left(\frac{1+w}{1-w} - 0.652\frac{d}{R_1}\right)^{-1} \quad (1)$$

where

$$P = \frac{\pi^4 \nu^2 (R_1+R_2)}{2\omega_1^2 d^3 R_1^3 \left(1 - \frac{R_2^3 w}{R_1^3}\right)(1-w)} \quad (2)$$

R_1 = radius of the inner cylinder.

R_2 = radius of the outer cylinder.

$d = R_2 - R_1$ = gap between the cylinders.

ν = kinematic viscosity of the fluid.

$\omega_1 = \omega$ = angular velocity of the inner cylinder.

ω_2 = angular velocity of the outer cylinder.

$w = \omega_2/\omega_1$ (lies between 0 and 1).

Taylor found that this criterion hold true for the gap ratio d/R_1 as high as 1/3. Hence the criterion may be applied to our cases where the greatest gap ratio was only 0.135.

In our case only the inner cylinder was rotating, $w = 0$, the criterion will be then reduced to

$$P = 0.0571\left(1 - 0.652\frac{d}{R_1}\right) + 0.00056\left(1 - 0.652\frac{d}{R_1}\right)^{-1} \quad (3)$$

where

$$P = \frac{\pi^4 \nu^2 (R_1+R_2)}{2\omega^2 d^3 R_1^3} \quad (4)$$

or

$$\left(\frac{\omega}{\nu}\right)^2 = \frac{\pi^4 (R_1+R_2)}{2P d^3 R_1^3} \quad (5)$$

The numerical calculation for our two cases is given in the following tables. All the dimensions of length are in

inches except when otherwise specified.

Table I

Case	R_1	d	d/R_1	P
1	7.875	1.0625	0.1350	0.0527
2	7.875	0.5313	0.0675	0.0551

Table II

Case	R_1+R_2	d^3	R_i^2	$(\omega/\nu)^2$	(ω/ν)	$RN_c=\frac{\omega R_1 d}{\nu}$
1	16.8125	1.200	62.0	208.0	14.45	121
2	16.281	0.150	62.0	1535	39.20	162

where RN_c is the critical Reynolds number for the instability of the flow in the corresponding case.

The operating range of the circumferential speed of the inner cylinder in our case is from U_i = 40.0 ft/sec. to U_i= 150 ft/sec. If we take ν= 0.0241 in^2/sec. = 1.675 x 10^{-4} ft^2/sec. which corresponds to barometric pressure 745mm Hg. at 22°C,(about the average atmospherical condition at Galcit), the operating range of Reynolds number $(RN)_{op}$ for our two cases will be given as in Table III

Table III

Case	d	$(RN)_{op}=\frac{U_i d}{\nu}$
1	1.0625	21100 to 79200
2	0.5313	10600 to 39700

From Table II and Table III we have the ratio of the operating Reynolds number to the critical Reynolds number for instability of laminar flow as given in Table IV.

Table IV

Case	d	$(RN)_{op}/(RN)_c$
1	1.0625	175 to 655
2	0.5313	66 to 240

From this calculation, we are justified in saying that the flow investigated was turbulent, because the operating Reynolds number was much larger than the critical Reynolds number.

Theoretical Discussion.

In turbulent motion, the relationship of turbulence to the mean flow is very important. The statistical effect of turbulence on the mean flow is similar to that of viscosity. Lumps of fluid carry its transferable properties from one layer to another just as molecular agitation transfers such properties as heat and momentum in a non-turbulent fluid. In these theories, a mixing length L plays a part analogous to the mean free path in molecular diffusion. Lumps of fluid leave their original neighbourhood and move in a direction transverse to the mean flow a distance L. At this point they mix with the surrounding fluid so that their properties becomes identical with the average properties of the fluid in that region.

Prandtl, in his momentum transport theory, assumed that the masses of fluid which transport the momentum of one layer to another move without being acted on by the transitory pressure gradients associated with turbulent motion. In the case of rotating cylinders, these fluid masses, acted on by the radial gradient of mean pressure, retain their moment of momentum about the axis of the cylinders.

Prandtl's expression for parallel flow (see Ref.11)

$$\frac{\tau}{\rho} = L^2 \frac{dU}{dy}\left|\frac{dU}{dy}\right| \quad \text{or} \quad k \frac{dU}{dy} \qquad (6)$$

is therefore replaced by

$$\frac{\tau}{\rho} = \frac{L^2}{r^2}\left(\frac{d}{dr}(rU)\right)^2 \qquad \text{or} \qquad \frac{k}{r}\frac{d}{dr}(rU) \qquad (7)$$

for the flow between rotating cylinders. Where $k\rho$ is the eddy viscosity. The couple about the axis due to the tangential stress τ over a cylindrical surface of radius r is independent of r. Hence

$$\frac{G}{\rho} = 2\pi rk\frac{d}{dr}(rU) = \text{constant} \qquad (8)$$

where Gl is the moment about the axis of reaction between the inner and outer cylinders and l is their length.

According to momentum transport theory $\frac{d}{dr}(rU)$ does not vanish anywhere in the space between the two cylinders and if the inner cylinder rotates and the outer cylinder is at rest, rU decreases continuously with increasing radius.

G.I.Taylor suggested that the fluid masses preserve their component of vorticity during the mixing process. When the mean motion is circular as is the case here, the component of vorticity, ζ, about the z-axis (the axis of the cylinders) may be expressed in cylindrical coordinates as

$$\zeta = \frac{1}{r}\frac{d}{dr}(rU) = \text{constant} = 2A \text{ (say)} \qquad (9)$$

$$rU = Ar^2 + B \qquad (10)$$

From Taylor's experimental results, by a special method of extrapolation, he found that the vorticity ζ is zero, i.e. rU is constant, over about 80% of the region between the cylinders (but not near to the walls).

So far we have considered that the flow between the concentric rotating cylinders is two dimensional. No similar extension to the three dimensional case can be made at the present time due to the complexity of the problem. However in case of three dimensional turbulent motion, if one neglects the shearing stress due to pure viscosity, the transfer of angular momentum at each section of radius r must be equal to the torque which is constant, i.e.

$$r^2(U + u + u')(v + v') = \text{constant} \qquad (11)$$

where U is the average mean circumferential velocity at radius r for all the axial positions; u is the deviation from the mean circumferential velocity at radius r at a given axial position; v is the radial velocity; u' and v' are the circumferential and the radial turbulent fluctuations respectively.

From the continuity of flow, the average of the term Uv taken over the whole length of the cylinders will be zero. Averaging over time and length in the axial direction one has from equation (11)

$$r^2(\overline{uv} + \overline{u'v'}) = \text{constant} \qquad (12)$$

This equation shows that the torque is transferred from one cylinder to the other by two different mechanisms : (A) secondary motion, and (B) turbulent fluctuations. The relative importance of these should be determined experimentally.

this, in fact, depends greatly upon the experimental arrangement

Experimental Results and Discussion.

1. Preliminary Investigations.

At first it was thought that the flow between the cylinders would be two dimensional except near the ends. Hence measurements were made at the exact center of the cylinders where the flow would best represent this two-dimensional type. However two entirely distinct types of flow were obtained at the same position depending on the starting conditions. The typical sets of the velocity and the turbulence distributions across tha gap for these two types are shown in Figs. 14 to 17. For convenience, let us call the type of flow shown in Figs. 14 and 16, "A", and that shown in Figs.15 and 17, "B". The main features of these flows are as follows:

For type "A" flow, there is a large boundary layer near the inner cylinder, i.e., the mean velocity decreases gradually from the inner cylinder toward the center of the gap. Beyond the center of the gap the mean speed increases slightly toward the outer cylinder until a very short distance from the wall is reached whence it decreases rapidly to zero at the wall. The turbulence decreases toward the outer cylinder and its magnitude is comparatively lower than for type B.

For flow of the type B, the mean velocity decreases rapidly from the inner cylinder outward to a certain minimum

value. Then it starts to increase slightly toward the outer cylinder until the maximum value is reached. Beyond the maximum point the mean velocity starts to decrease gradually toward the outer wall. Hence there is a large boundary layre near the outer cylinder wall and a small one near the inner wall. The intensity of turbulence is higher near the outer wall and decreases gradually toward the inner one.

The relation of these two types of flow to the starting conditions is given below:

If we started the inner cylinder in such a manner that we increased its speed gradually up to the desired value and if the hot-wire spindles were close to the inner cylinder, type A flow was obtained. On the other hand, if we started with the hot-wire spindles close to the outer cylinder and increased the speed to a fairly high value at once and then brought it down to the desired value, type B flow was obtained. Once either type of flow was established it seemed unaffected by slight changes in rotating speed.

Furthermore at higher speed it was found that in the middle of the run, the type A flow might suddenly change to the type B flow. This is illustrated in Fig.18. At first we started the cylinders in such a way that the type A flow was obtained, and took readings outward. These followed the upper full-line curve as shown in Fig.18, At certain point near the outer wall, the mean speed dropped suddenly along

the dotted line and then the velocity distribution became that shown in the lower full-line curve, i.e. type B flow. Further traversing had no effect. When the 17/32" gap was used, decreasing the rotating speed of the inner cylinder to a certain low value restored the type A flow, however for 1-1/16" gap this did not occur.

The explanation for the above phenomena may be one of the following: It might be due to the fact that the spindles of the hot-wire produced a thick boundary layer on the cylinder wall during starting. Or the flow in the rotating cylinders was not two dimensional so that some special transition caused the above phenomena.

At first the inner cylinder was not sealed and it was possible that circulation from its interior into the gap occurred. Hence we decided to seal the inside of the inner cylinder by wooden plates so as to eliminate the possibility of such a secondary flow. However such a seal did not change the experimental results in any noticable manner, so that probably no undesirable secondary flow existed in the cylinders.

As to the possibility of producing a thick boundary layer on the surface of the cylinder wall by the hot-wire spindles, a dummy hot wire was inserted into the rotating cylinders at the same axial position but 180° from the real hot-wire. It is shown in Fig.7. The velocity distributions

across the gap obtained by starting the rotating cylinders with different positions of the dummy and the real hot-wires in the gap, are shown in Fig.19. In genral these two distinct types of flow still existed. The transition phenomenon was not due to the production of a thick boundary layer by the hot-wire spindles during starting.

In order to determine the flow pattern in the gap of the cylinders, a few evenly spaced orifices were first inserted on the outer cylinder along the axial direction. The readings of these orifices showed that the static pressure was not constant along the axial direction as would be expected in case of two dimensional flow, but varied up and down. This gave some indication that the flow was not two-dimensional but that certain peculiar secondary motion existed there.

It was found that the end conditions of cylinders have considerable influence on the static pressure readings. At first the end conditions were not same and it appeared desirable to make them so. Several means were tried. The results showed that the end conditions did effect the velocity distribution across the gap even at the middle point of the cylinders where our measurements were taken. However the types of flow still existed. The final system adopted was that described on page 3.

For the 1-1/16" gap, the aspect ratio, i.e. the ratio

of the length of the working section to the width of the gap is only about ten to one. For such an aspect ratio, the end effects on the flow at the mid-point might be considerable. Hence we repeated the measurements with 17/32" gap, increasing the aspect ratio by two, in ordre to reduce any effect that did exist. However the results obtained with the 17/32" gap were essentially the same as those obtained with the 1-1/16" gap, and we felt that the end effects were negligible at the place where our measurements were taken.

In order to see whether the flow was two- or three-dimensional, the measurements at different axial positions were made. For the same starting condition and the same static pressure distribution, it was found that at different axial positions, the velocity distribution across the gap is different. Hence we knew that the flow was really three dimensional. An extensive investigation was then carried out. The number of the static pressure orifices was increased to fifteen, as shown in Fig.7. As a result, a qualitative idea of the flow pattern in the gap along the axial direction could be obtained.

2. Behavior of the Static Pressures.

In case of two-dimensional flow the variation of static pressure across the gap of the cylinders can be calculated. Let U be the circumferential velocity at a radius r from the center of the cylinder. Then the pressure gradient along r

must be in equilibrium with the centrifugal force.

$$\frac{dp}{dr} = \rho \frac{U^2}{r} \qquad (13)$$

It would have been difficult to measure the static pressure at the wall of the inner rotating cylinder. Since the static pressure p_s at the outer stationary cylinder could easily be obtained, the difference in static pressure between the two cylinders was roughly estimated by the help of equation (13).

The mean level of the static pressure cannot be determined mathematically, because we do not know the exact limits over which equation (13) should be integrated. It was found that the level of the static pressure at the outer wall was determined by two factors. One was the end conditions and the other was the speed of the inner cylinder. We measured the static pressure with the atmospheric pressure as reference. It was higher than the atmospheric at the outer wall and its value increased as the square of the speed of the inner cylinder. At first the ends of the rotating cylinders were closed very tightly as shown in Fig.1-A. The level of the static pressure was very high. A typical distribution curve for this case is shown in Fig.20. The variation is seen to be of the same order as the pressure difference between the inner and the outer walls as estimated by equation (13). Several different ends arrangement were tried, each of which gave a different level of static pres-

sure. However the variation with the axial position still existed and the value still increased with the square of the rotating speed of the inner cylinder. The arrangement finally used gave a very low mean static pressure, its distributions curves are shown in Fig.21.

From Fig.21, one point is noticable; that the peaks are approximately equi-distant. As we know that along the wall flow must occur from the high to lower pressure regions, this diagram indicates that there was a secondary flow such as ring-shaped vortices. It is worthwhile to note that the distribution shwon in Fig.21 corresponds to the atarting conditions which gave type A flow in the preliminary investigations.

3. Investigations along the Axial Direction of the Cylinders.

From the distribution of the static pressure as shwon in Fig.21, we knew that the flow was three dimensional. Hence we investigated the velocity and the turbulence distributions at various axial positions in order to obtain a better understanding of the phenomena. Since the flow pattern could be changed by the starting conditions, care had to be exercised that the static pressure distribution along the axial direction was kept the same for all the runs at any given speed.

The results are shown in Fig.22 to Fig.30. Investiga-

tions were made at three different speeds of the inner rotating cylinder, i.e. 960, 1200, 1500 r.p.m. Measurements were taken at seven axial stations at the central portion of the cylinders. The distance between the two adjoining stations was 1/2". Hence the total axial distance investigated was 3". Let us number these stations from 1 to 7; the number increasing towards the bottom of the cylinders. The actual positions of these stations are marked by the arrows in the static pressure diagrams on the right of the corresponding results.

Now let us take the results for 1200 r.p.m. as a typical set and analyze them in detail.

The mean velocity distributions for this case are shown in Fig.22. It is seen that both types of flow obtained in the preliminary investigations existed simultaneously for the same flow pattern, but at different axial positions. The mean velocity distribution changes from one type to the other, gradually. For instance, at station No.1 the distribution is type B; at stations No.2 and No.3, it is type A; at station No.4, it is an intermediate type, we will call it A_B; at stations No.5 and No.6, it is type B again; while at station No.7, the intermediate stage is again obtained.

If we plot one of the distribution of type A, say at station No.2, and one of type B, say at station No.6,

on semi-logarithmic paper, we obtain Figs. 31 and 32 respectively. From these curve we see that for flow of type A, the velocity distribution near the inner wall is logarithmic, while for type B, the velocity distribution near the outer wall is logarithmic, i.e. $U_i - U = \text{const.} \times \log y$, where y is the distance from the wall. If we plot the typical velocity distribution obtained in the preliminary investigations in the same manner, the results are similar, see Figs. 33 and 34. It was shown by Prof. von Karman in his paper "The Fundamentals of the Statistical Theory of Turbulence" that for Couette's flow, the mean velocity distribution is logarithmic if homogeneous turbulence is assumed. It may be stated that at the place where the velocity distribution is logarithmic, the transfer of shearing stress from one cylinder to the other is mainly by the turbulent fluctuations.

From equation (12) we have

$$r^2(\overline{uv} + \overline{u'v'}) = \text{constant} \qquad (12)$$

Since the gap is small in comparison with both radii of the cylinders, by first approximation we have

$$\overline{uv} + \overline{u'v'} = \text{constant} \qquad (14)$$

At the place where the influence of the secondary motion, i.e. the term of $\overline{uv}$ is negligible we have

$$\overline{u'v'} = \text{constant} \qquad (15)$$

This is also the condition for Couette's flow, in which the velocity distribution is logarithmic.

At the place where the influence of turbulent fluc-

tuations is small we have

$$\overline{uv} = \text{constant} \qquad (16)$$

We did not attempt to measure the radial velocity v of the secondary motion. However we can draw some conclusions as to the distribution of v along the axial direction from equation (16), after examining the distribution of u ,i.e., the deviation of the circumferential velocity from the average value along axial direction.

First we take an average of the mean velocity curves of the seven stations. This average mean velocity distribution is plotted as dotted curves on the mean velocity distribution curves of Fig.22. The differences between these curve give the distribution of u at various axial positions, as shwon in Fig.23.

From equation (16) we know that the signs of u and v should be the same. But from Fig.23 we see that for flow of type A, u is positive, and that for type B, u is negative. Hence we conclude that the radial component of the velocity of the secondary motion,v, changes its direction at different axial position.

It seems therefore that ring-shaped vortices which are known to introduce the instability of the flow in rotating cylinders still exist at Reynolds numbers as high as several hundreds times the critical Reynolds number. In order to give satisfactory explanation of the experimental

results, these ring-shaped vortices must be assumed to be distorted and arranged as shown in Figs. 35 and 36. (cf. Fig.13 which is Taylor's original conception of the vortices). Since the fluid along the walls diverges from stations No.3 and from somewhat beyond No.7, the static pressure has peaks at these points. The static pressure drops in the neighbourhood of stations No.3 and No.7 rather rapidly and over the mean portion of the interval between the two peaks is more or less constant. This is also consistent with the suggested distribution of vortices. Opposite to the stations No.2 and No.3, near the inner cylinder there is a turbulent domain; this explains why we get the flow of type A. In this turbulent domain we expept the velocity distribution to be logarithmic; this has been found to be correct. At stations No.5 and No.6, i.e. between the vortices, there is a turbulent domain near the outer cylinder wall; this results in the flow of type B. At stations No.4 and No.7, the intermediate stage will be obtained because the influence of the secondary motion and that of the turbulent fluctuations are of the same order of magnitude.

The level of the mean velocity of the type A flow is higher than that of Type B, because the flow of type A is associated with a positive radial velocity v and a positive u; while negative v and u will be associated with type B flow.

Very close to the walls, the shear should be mainly determined by pure viscosity. In order to transmit the same amount of shear as exists in the central portion of the gap, the slope of the velocity curve near the walls must be enormously large. In all the velocity curves that we obtained, this is true.

The distributions of u', the circumferential turbulent fluctuations, are shown in Fig.24. It is interesting to note that the curvature of the distribution curves for u and u' are opposite for any given axial stations.

Figs. 25 to 27, in sequence, show the mean velocity distributions, the deviations of the circumferential velocity from the average value, and the circumferential turbulent fluctuations, at various axial positions; all for a speed of 960 r.p.m. Figs. 28 to 30 are a similar series for 1500 r.p.m. The general features of these curves are similar to those obtained at 1200 r.p.m. which we have just discussed.

If we reduce the average mean velocity distributions for the three speeds into non-dimensional form, we find that they are very close to each other. One curve, Fig.37, may represent all of them. In Fig.38, this final average mean velocity curve is plotted on semi-logarithmic paper. From these curves we see that the average mean velocity is constant over about 60% of the region between the cylinders, but not near to the walls. The curve is symmetrical about

the middle of the gap, however even in the region where the average mean velocity is variable its distribution is not logarithmic. This can be expected, because the term $\overline{uv}$ resulting from the secondary motion is variable over the gap. It can be assumed that in the center portion of the gap the momentum is transferred entirely by the secondary motion.

The relative position of the vortices in the axial plane is influenced somewhat by the end conditions of the cylinders. As we changed the end conditions, the static pressure distribution curve changed too. However the existance of the vortices is not affected by the end conditions because no matter what these were the general character of the experimental results remained the same.

As to the relation of the vortices to the rotating speed of the inner cylinder the following facts were found:

Measurements at a fixed axial position but with different rotating speed were made, see Fig.39,. The procedure was as follows:

Running at the low speed of 1200 r.p.m. we obtained the curve shown on the top of Fig.39, i.e. diagram 1. It shows essentially a flow of type A. Then we increased the speed to 1500 and 1800 r.p.m. The results are given as in diagrams 2 amd 3 of Fig.39 respectively. The distribution of the static pressure as well as the distribution of mean velocity are more or less similar to those of diagram 1.

Now we further increased the speed to 2100 r.p.m. Then the distributions of static pressure and of velocity were suddenly changed, as shown in diagram 4 of Fig.39. The pressure peak that existed in the three preceding cases at the midpoint where the measuremants were taken, disappeared and thus the mean velocity distribution at thispoint became type B. When again we reduced the ro tating speed to 1800 and 1500 r.p.m., diagrams 5 and 6 in Fig.39 were obtained. They are similar to diagram 4, which shows that the new flow pattern, once established, continued after a considerable reduction of the speed. But as we decreased the rotating speed to 1200 r.p.m., the original flow pattern returned, as shown in diagram 7 of Fig.39.

It seems that at lower speed there was a certain stable configuration of the size and the number of the vortices. As the speed was increased, a critical value was reached when the vortices increases in size and decreases in number. Since the vortices can exist only in pairs, because the total circulation must be zero, a pair of vortices may disappear at a ceratin critical speed as the speed increases, and reappear at some other critical speed as the speed decreases. There is no reason why these two critical speeds should be the same. This mechanism explains fully the sudden changes of flow encountered in the preliminary investigations. The effect of the position of the spindles was

that if the spindles were in the place where the secondary motion predominated, they would prevent the formation of such vortices. Hence during starting the spindles had to be placed in the turbulent domain, this is consistent with the experimental results.

We had only two stable vortex-systems in our operating range. Let us call the one which prevails at lower speed, the small-vortex-system, and that existing at high speed, the large-vortex-system. For 17/32" gap the upper critical speed of the small-vortex-system was found at 1800 r.p.m. or higher. Hence we can say that the upper limit of the critical Reynolds number for the existance of the small-vortex-system is about 200 times the critical Reynolds number for instability of the laminar flow. Beyond this limit only the large-vortex-system can exist. The lower limit of the critical Reynolds number for the large-vortex-system,(i.e. at 1200 r.p.m. or lower), is about 100 times that of the critical Reynolds number for instability of the laminar flow. Below this limit only the small-vortex system can exist. There is a range in which both types of the flow pattern can exist and it depends on the starting conditions which pattern prevails in a particular case. For 1-1/16" gap the lowest operating Reynolds number is about 175 times that of the critical Reynolds number so that we could not change from the large-vortex-system to the small-

one, if the large-vortex-system was once established.

Due to the mechanical limitation of the present equipment, we can not operate the rotating cylinder at very high speed. It would be interesting to rebuild the whole equipment so that it can be operated at a speed ten or more times the present highest value and make the cylinders two or three times longer so that more vortices may be obtained. Then a thorough investigation of the relation between the vortices and the rotating speed of the cylinder could be made. One more thing should be done in further investigation of the flow between rotating cylinders; a method should be found for determining the radial and the axial components of the secondary motion and of the turbulent fluctuations. In the present investigations by the hot-wire anemometer we could not determine the direction of the flow nor any other velocity components but those in the direction of the main flow. If the other components of the secondary and the turbulent motion were determined, the behavior of the vortices would be more thoroughly understood.

Though it is evident that the two-dimensional theories we discussed before can not be applied directly to these three dimensional motion of the ring-shaped vortices, it is interesting to compare these theories with the actual flow. The Ur curves for the two typical distributions A and B are shown in Figs. 40 and 41 respectively. It is seen

that the Ur neither decreases with the increase of r as predicted by Prandtl's theory, nor is constant as predicted by G.I.Taylor. Hence these theories can not be used even as first approximation.

Conclusions.

Measurements of pressure and velocity distributions in the flow between coaxial rotating cylinders where the inner cylinder rotates and the outer one is at rest show the following general results:

1. Hot-wire measurements of the velocity distribution between the cylinders show that the mean velocity in certain section increases with increasing radius. Since the "shadow effect" of the measuring device, suggested by G.I.Taylor, did not exist in the present case, such velocity distributions must be explained by assuming a secondary motion.

2. The analysis of the velocity distribution across the gap and the pressure distribution along the outer wall leads to the conclusion that ring-shaped vortices which are known to introduce the instability of the laminar flow exist at a Reynolds number as high as several hundred times the critical Reynolds number for instability, but their shapes are somewhat distorted.

3. Due to the existance of the ring-shaped vortices there are two main types of distribution of velocity and turbulence across the gap between the cylinders. These are due to the different directions of the radial flow and the relative contributions of the secondary motion and the turbulent fluctuations to the transfer of the shearing

stress.

4. In regions where the secondary flow is negligible, the flow between rotating cylinders with small gap can be approximated by the flow of the Couette type and the mean velocity distribution is logarithmic.

5. The static pressure is not constant along the axial direction of the cylinders because of the secondary motion. The mean level of the static pressure in the rotating cylinders is mainly determined by the end conditions. For a given end conditions, the value of the static pressure increases with the square of the speed.

6. The size of the vortices and their number depend on the speed of the inner cylinder. The vortices can only exist in pairs. A certain critical speeds, the vortices may suddenly loss or gain a pair, and a big change in the flow pattern occurs. In general at high speeds the number of the vortices tends to decrease and their size increases. In certain speed range either of the two different arrangements may exists, depending on the starting condition of the system.

7. Further research to determine the radial and the axial components of the velocity and the turbulent fluctuations is necessary in order to analyze thoroughly the nature of the vortex-ring-system.

References.

(1) Taylor, G.I.: Stability of a Viscous Liquid Contained between Two Rotating Cylinders.
Phil. Trans. Roy. Soc. A,223 (1923) p.289.

(2) Taylor, G.I.: Distribution of Velocity and Temperature between Concentric Cylinders.
Proc. Roy. Soc. London A, No.874, Vol.151, P.492-512. Oct. 1935.

(3) Taylor, G.I.: Fluid Friction between Rotating Cylinders.
Proc. Roy. Soc. London A, No.892, Vol.157, p.546-578. Dec. 1936.

(4) von Karman, Th.: Some Aspects of the Turbulence Problem.
Proc. of 4th Intern. Congress for Appl. Mechanics.
p.54 - 91.

(5) von Karman, Th.: The Fundamentals of the Statistical Theory of Turbulence.
Journal of the Aero. Sci., Feb. 1937.

(6) Wattendorf, F.L.: A Study of the Effect of Curvature of Fully Developed Turbulent Flow.
Proc. of Roy. Soc. London A, No. 865, Vol.148, p.565-598. Feb. 1935.

(7) Dryden H.L. and Keuthe A.M.: The Measurement of Air Speed by the Hot-Wire Anemometer.
NACA TR. 320, 1929.

(8) Dryden H.L.: Turbulence and the Boundary Layer.
Journal of the Aero. Sci., Jan. 1939.

(9) von F. Wendt: Turbulente Stromungen zwischen Zwei Rotierenden Konnaxialen Cylindern.
Ingenieur Archiv, Vol.4, 1933, p.577-595.

(10) Goldstein S.: Modern Developments in Fluid Dynamics.

(11) Durand W.F.: Aerodynamic Theory, Vol.III, Division G.

(12) Knoblock F.D.: Investigations of the Application of the Hot-Wire Anemometer for Turbulence Measurements.
Ph.D. Thesis, Calif. Inst. of Technology, 1939.

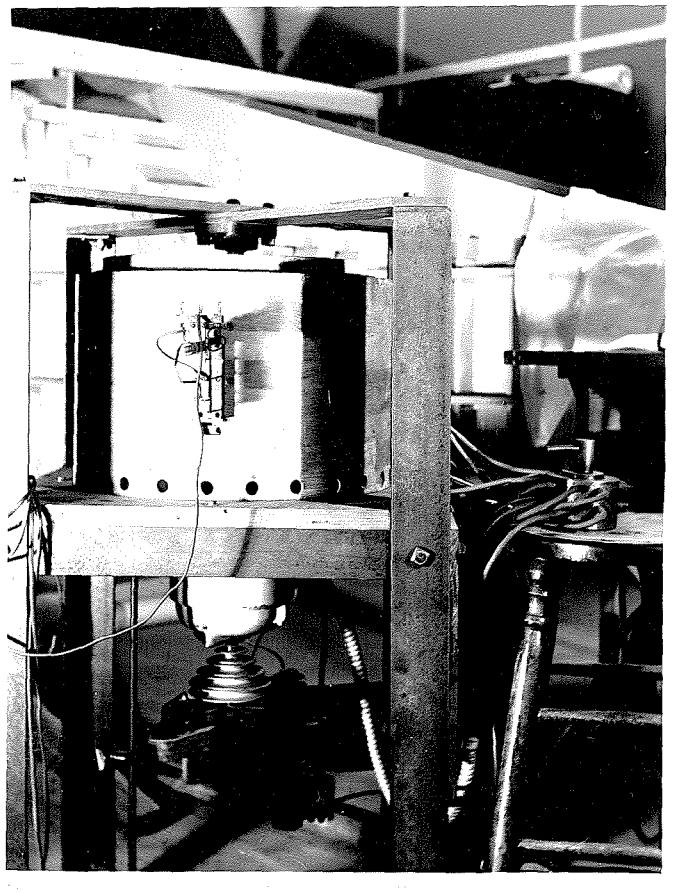

Plate I - Cylinders

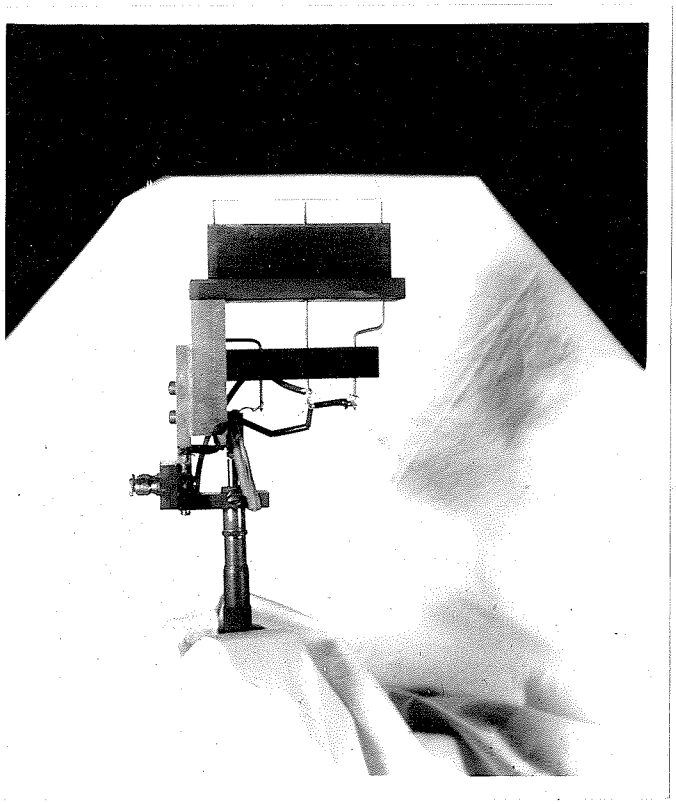

Plate II - Hot Wire Holder, showing two hot-wires used to measure at two axial stations simultaneously.

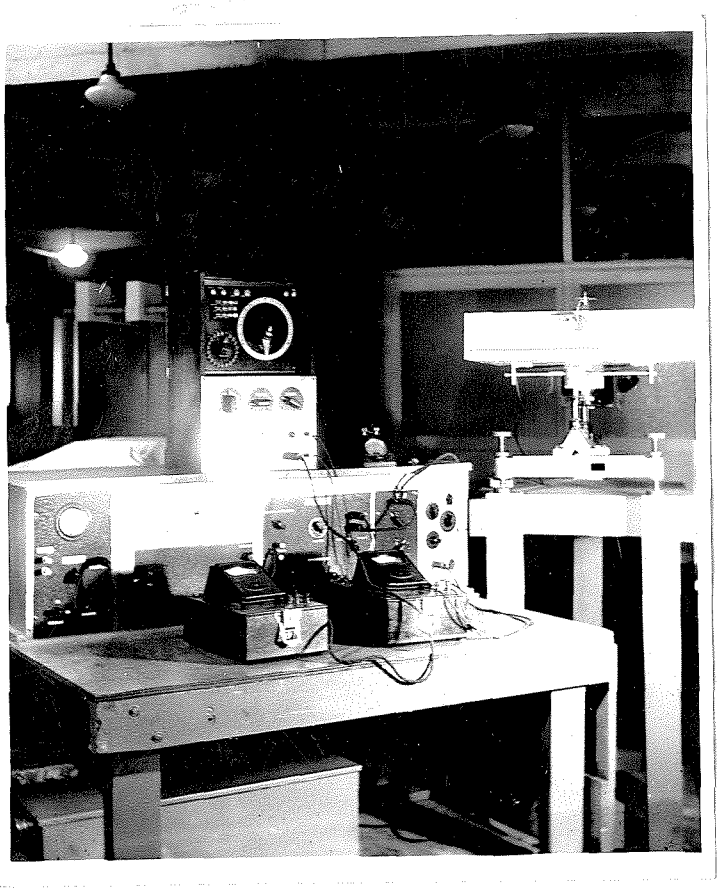

Plate III - Hot Wire Anemometer

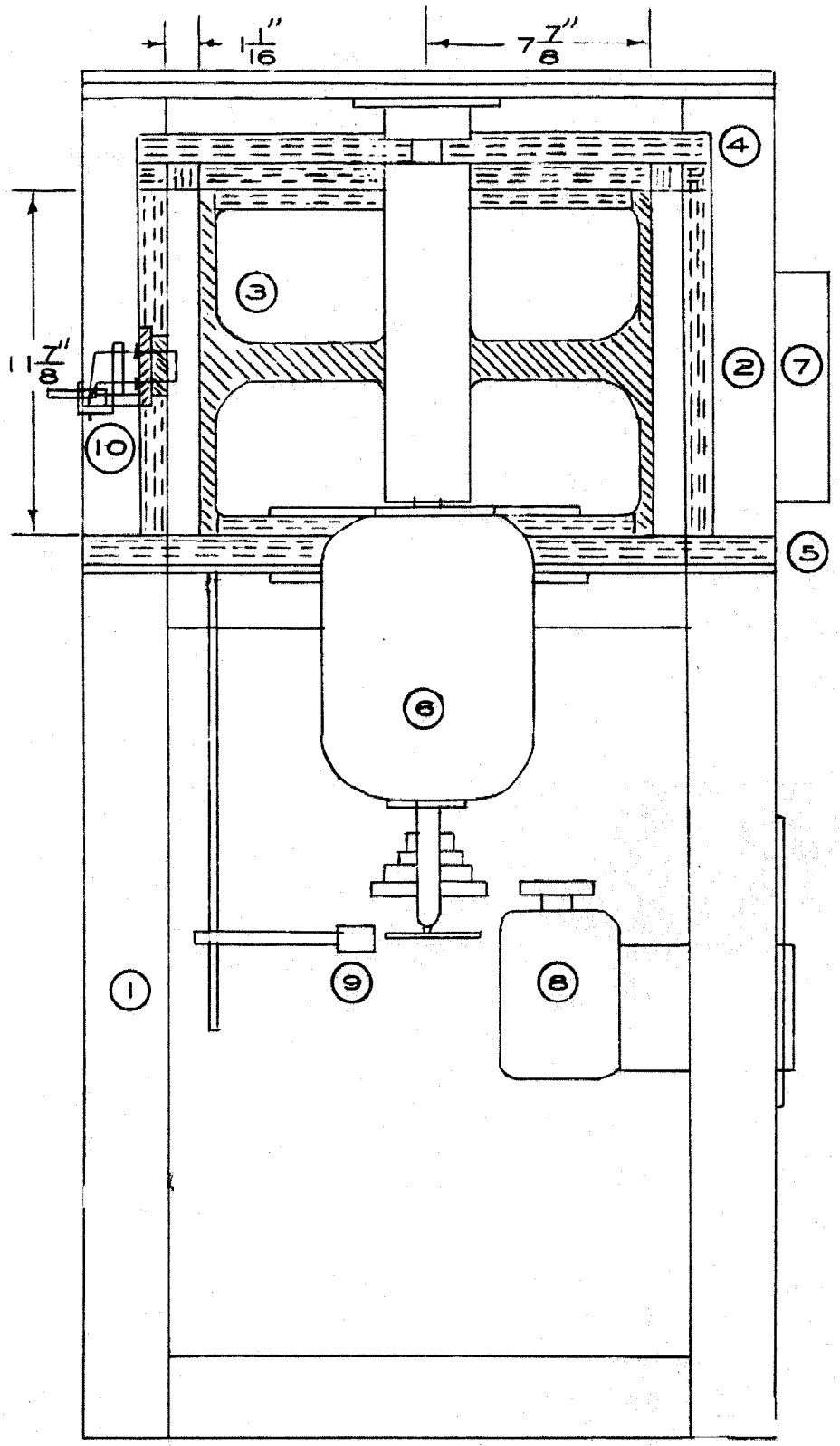

FIG1-ASIDE VIEW OF CYLINDERS

1 1/16" GAP SHOWN

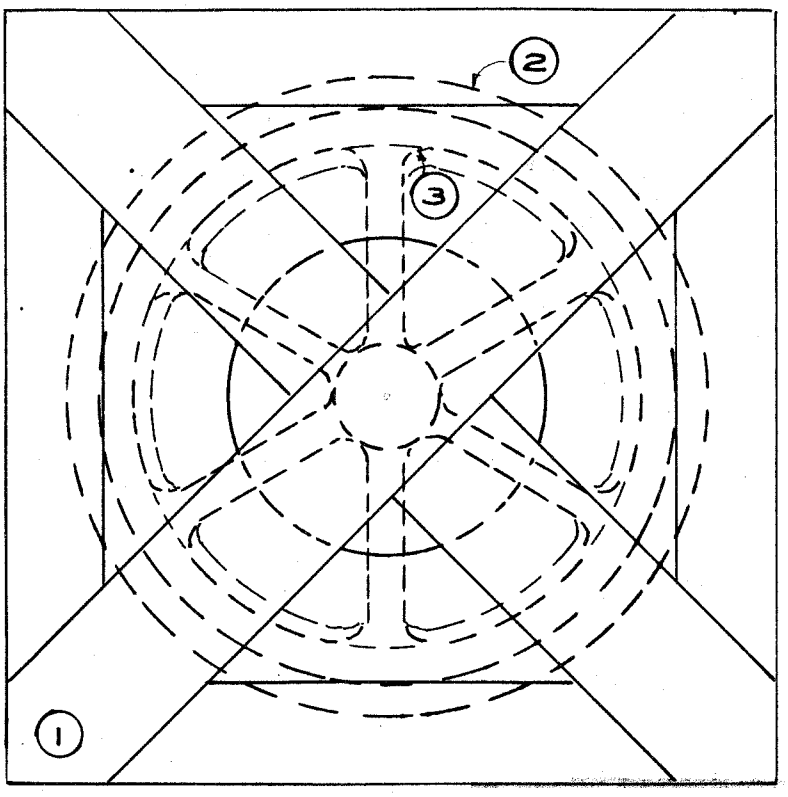

FIG i-B TOP VIEW OF CYLINDERS

1. FRAME
2. OUTER CYLINDER
3. INNER CYLINDER
4. TOP PLATE
5. BOTTOM PLATE
6. SYNCHRONOUS MOTOR
7. SWITCH FOR SYNCHRONOUS MOTOR
8. D.C. MOTOR WITH PULLEYS
9. PICK UP UNIT
10. HOT WIRE HOLDER

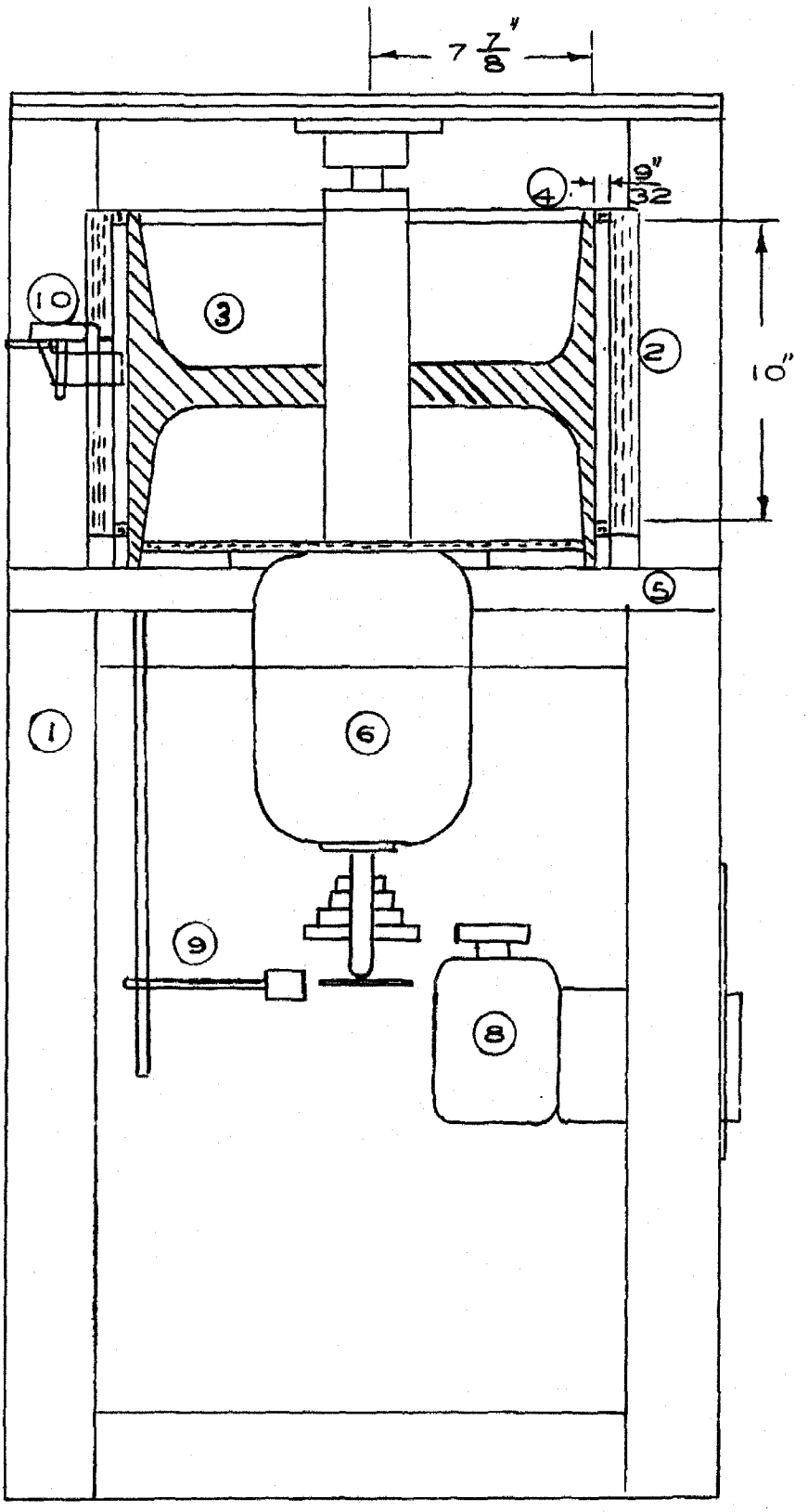

FIG. 1-C -SMALL GAP CYLINDERS

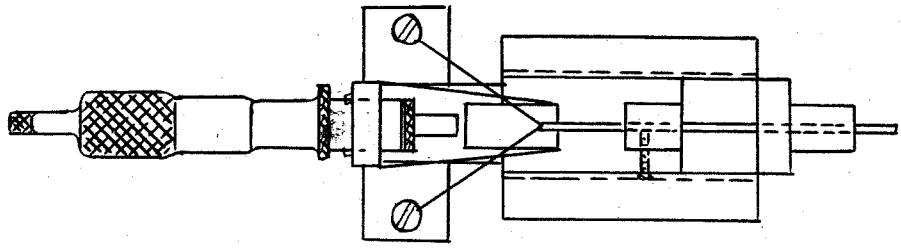

TOP VIEW

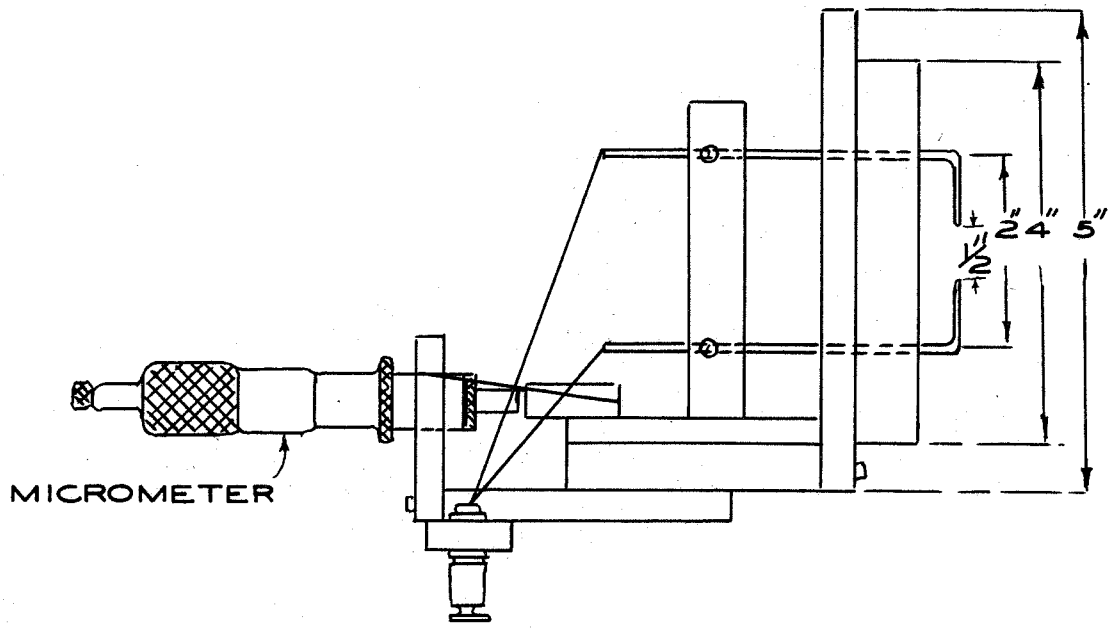

SIDE VIEW

FIG. 2 HOT-WIRE HOLDER

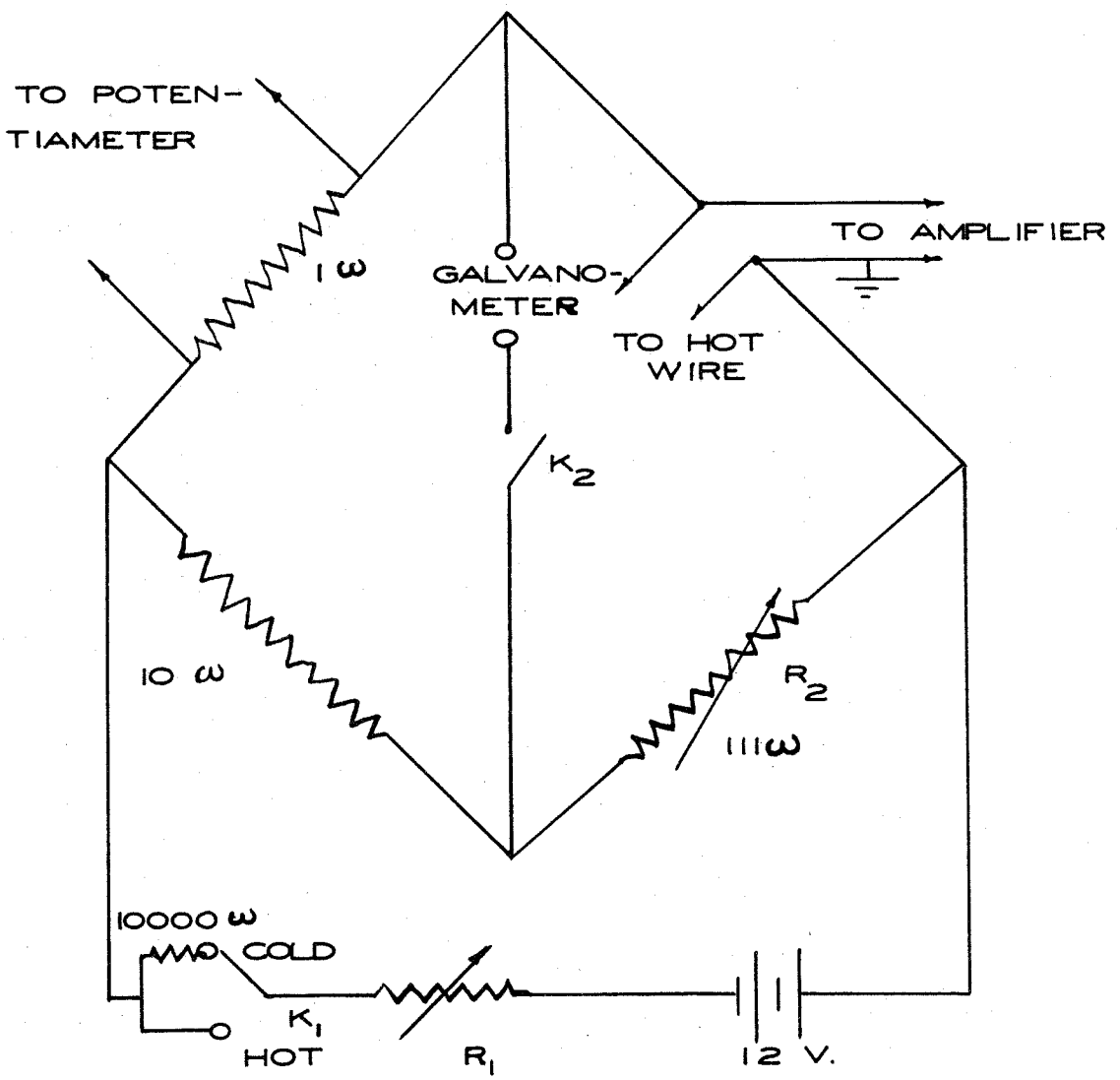

FIG. 3 – HEATING CIRCUIT OF ANEMOMETER

NO. 2

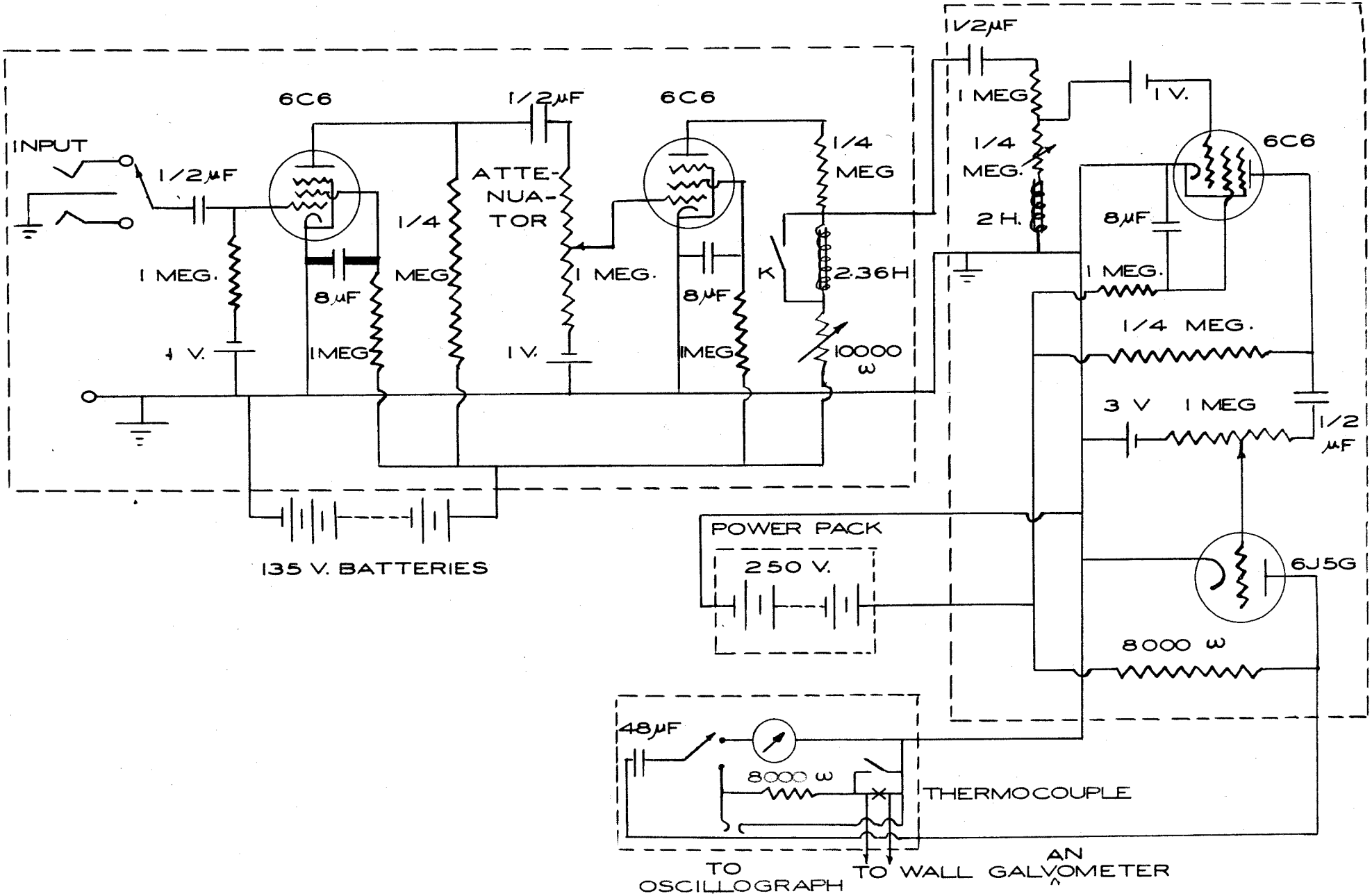

FIG. 4 - AMPLIFIER OF HOT WIRE ANEMOMETER NO. 2

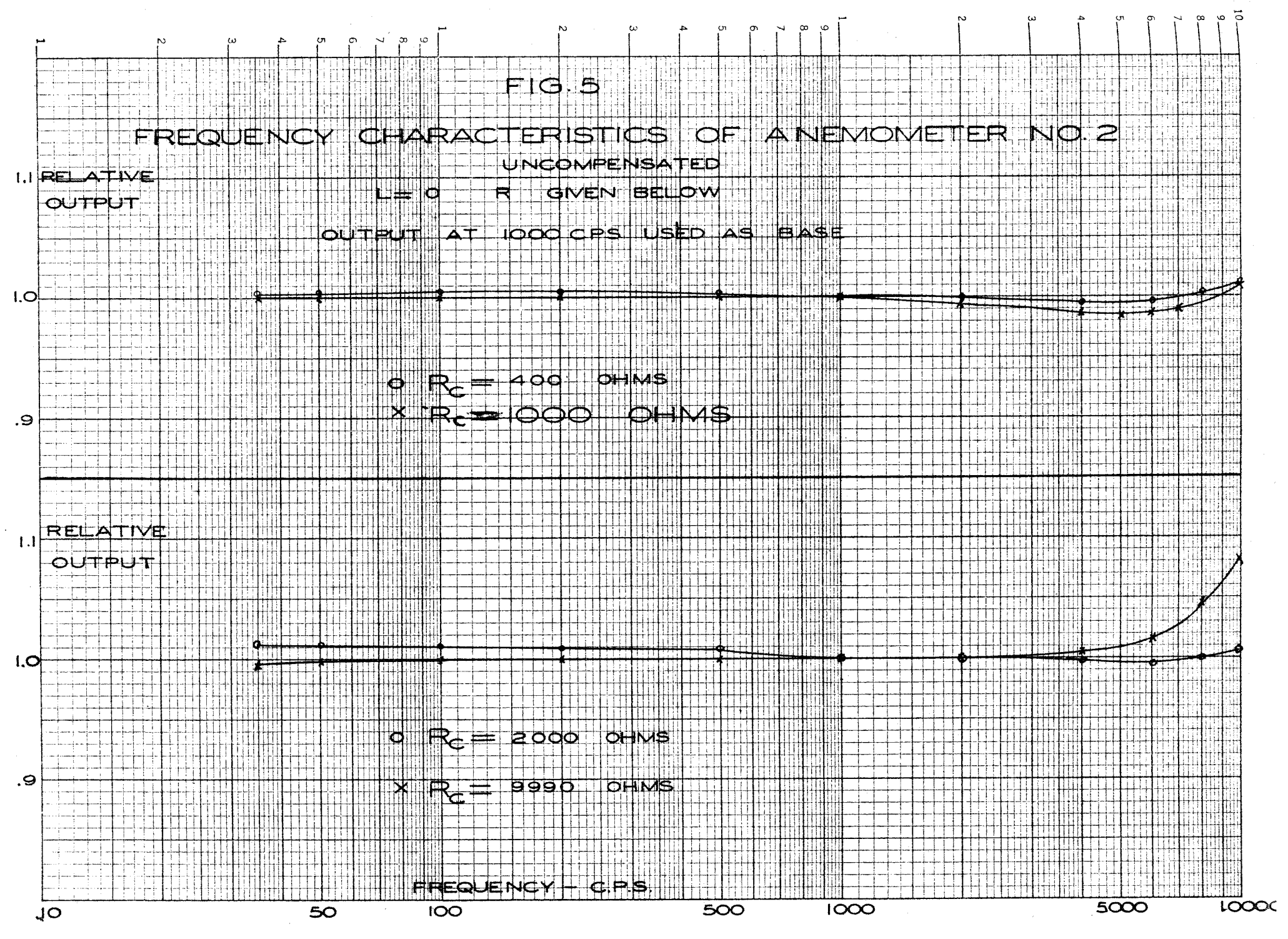
FIG. 5
FREQUENCY CHARACTERISTICS OF ANEMOMETER NO. 2
UNCOMPENSATED
L = 0 R GIVEN BELOW
OUTPUT AT 1000 CPS USED AS BASE
RELATIVE OUTPUT
1.1
1.0
.9
o R_C = 400 OHMS
x R_C = 1000 OHMS
RELATIVE OUTPUT
1.1
1.0
.9
o R_C = 2000 OHMS
x R_C = 9990 OHMS
FREQUENCY — C.P.S.
10
50
100
500
1000
5000
10000

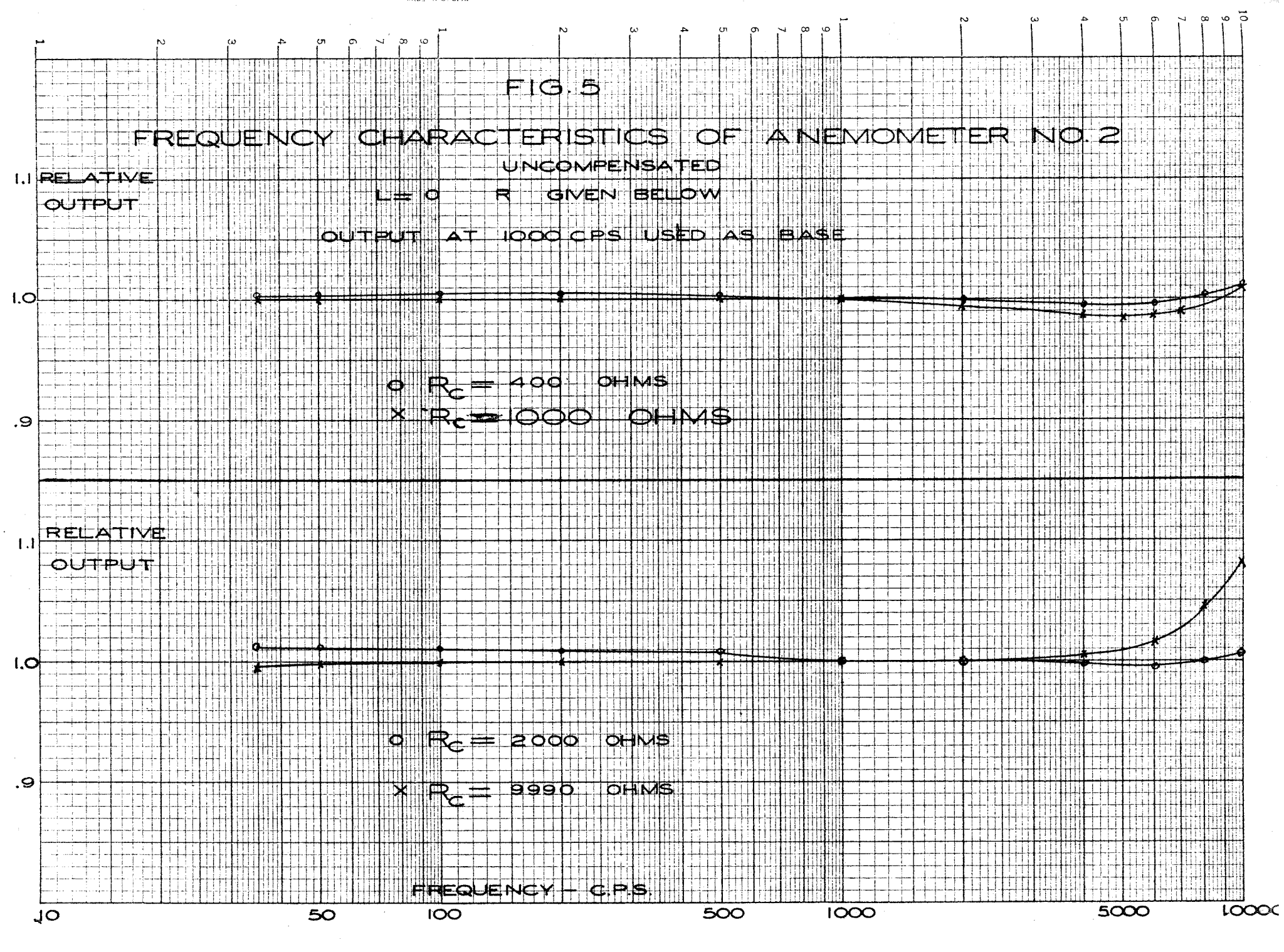
FIG. 5
FREQUENCY CHARACTERISTICS OF ANEMOMETER NO. 2
UNCOMPENSATED
L = 0 R GIVEN BELOW
OUTPUT AT 1000 CPS USED AS BASE
RELATIVE OUTPUT
1.1
1.0
.9
○ R_C = 400 OHMS
× R_C = 1000 OHMS
RELATIVE OUTPUT
1.1
1.0
.9
○ R_C = 2000 OHMS
× R_C = 9990 OHMS
FREQUENCY — C.P.S.
10
50
100
500
1000
5000
10000

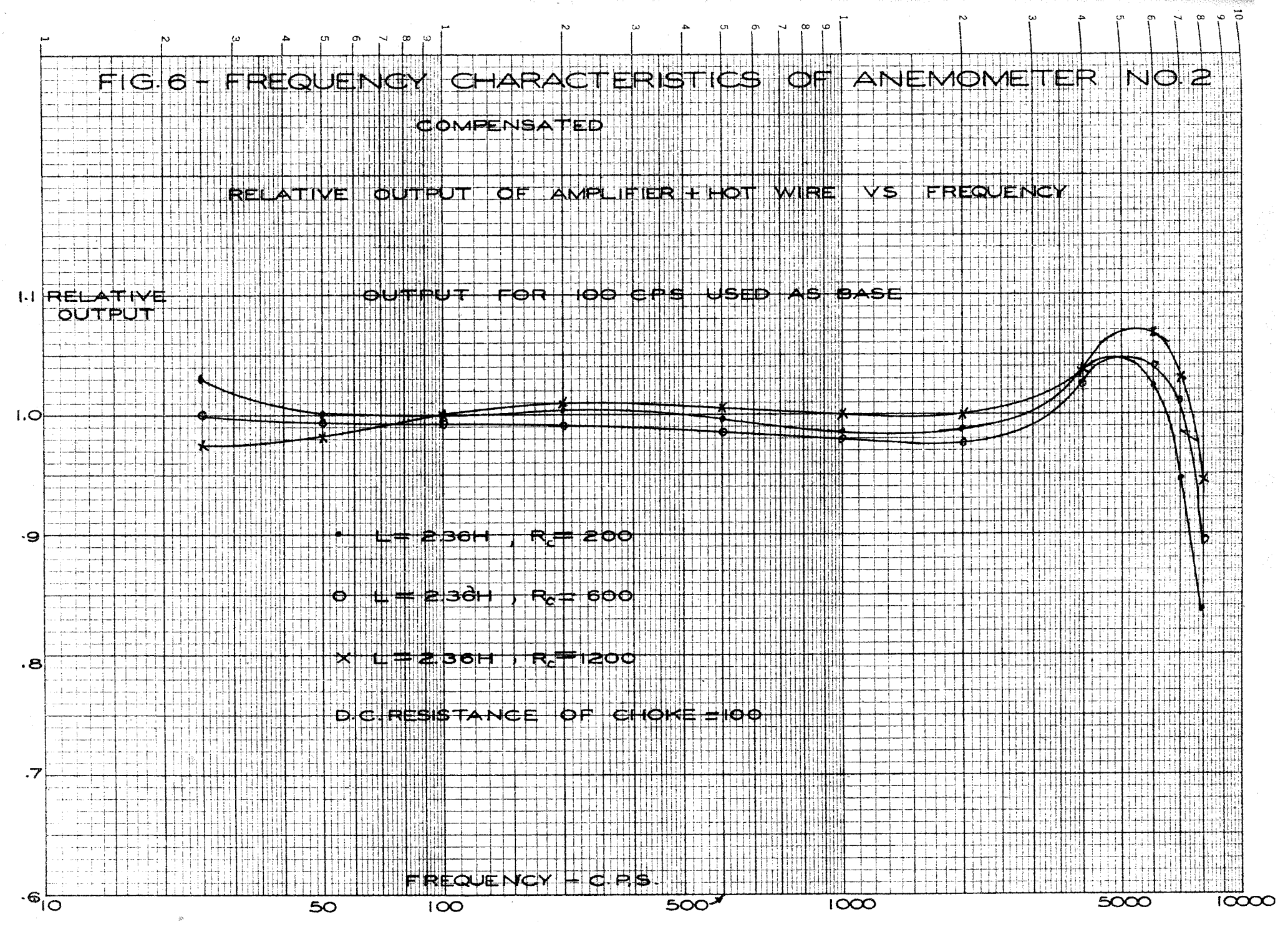
FIG. 6 - FREQUENCY CHARACTERISTICS OF ANEMOMETER NO. 2
COMPENSATED
RELATIVE OUTPUT OF AMPLIFIER + HOT WIRE VS FREQUENCY
RELATIVE OUTPUT
OUTPUT FOR 100 CPS USED AS BASE
1.1
1.0
.9
.8
.7
.6
• L = 2.36H , Rc = 200
o L = 2.36H , Rc = 600
× L = 2.36H , Rc = 1200
D.C. RESISTANCE OF CHOKE = 100
FREQUENCY - C.P.S.
10
50
100
500
1000
5000
10000

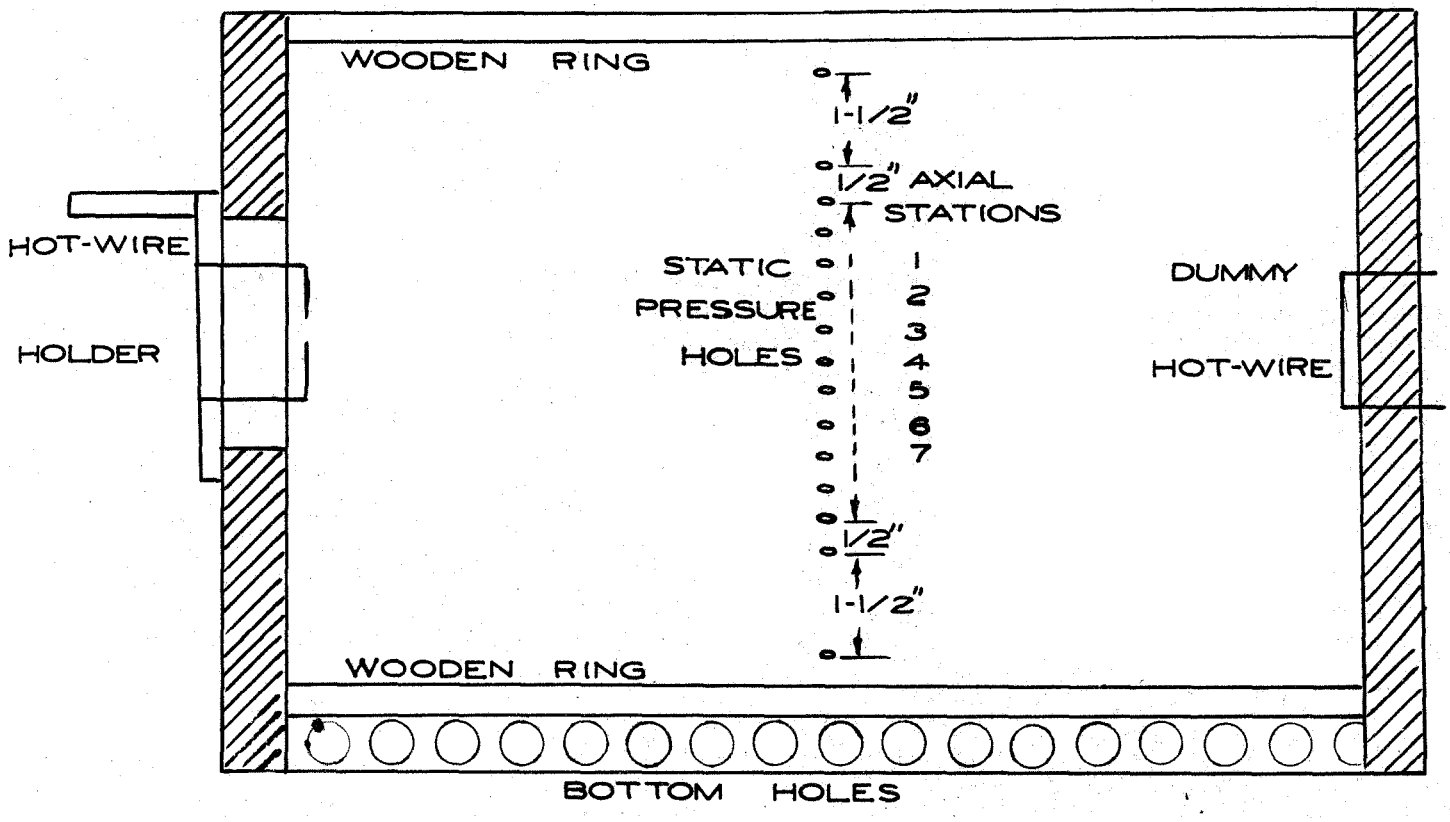

FIG. 7 – A SECTION VIEW OF OUTER CYLINDER

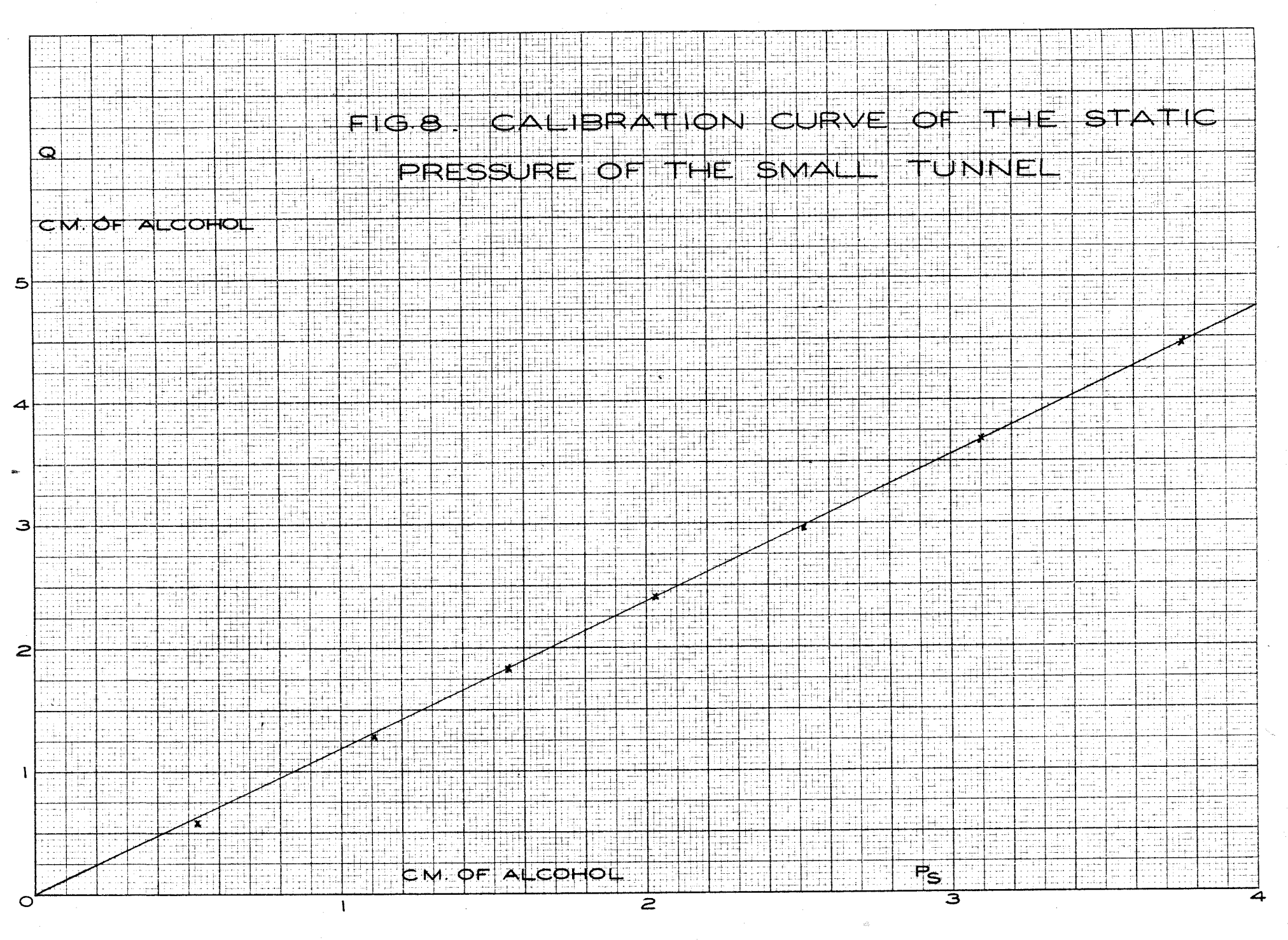
FIG.8. CALIBRATION CURVE OF THE STATIC PRESSURE OF THE SMALL TUNNEL
Q
CM. OF ALCOHOL
5
4
3
2
1
0
1
2
3
4
CM. OF ALCOHOL
P_S

FIG. 9 – A TYPICAL CALIBRATION CURVE OF HOT WIRE

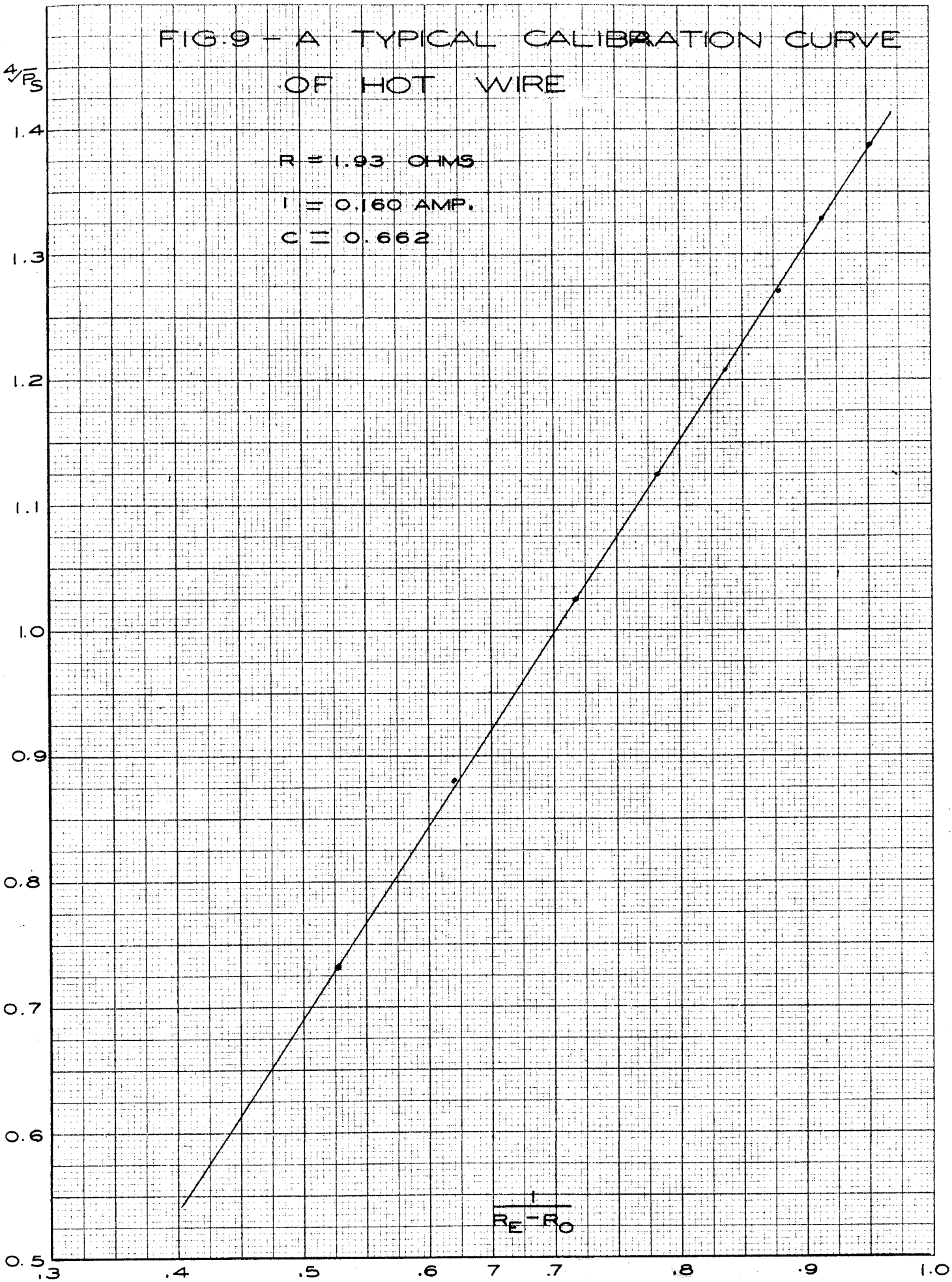

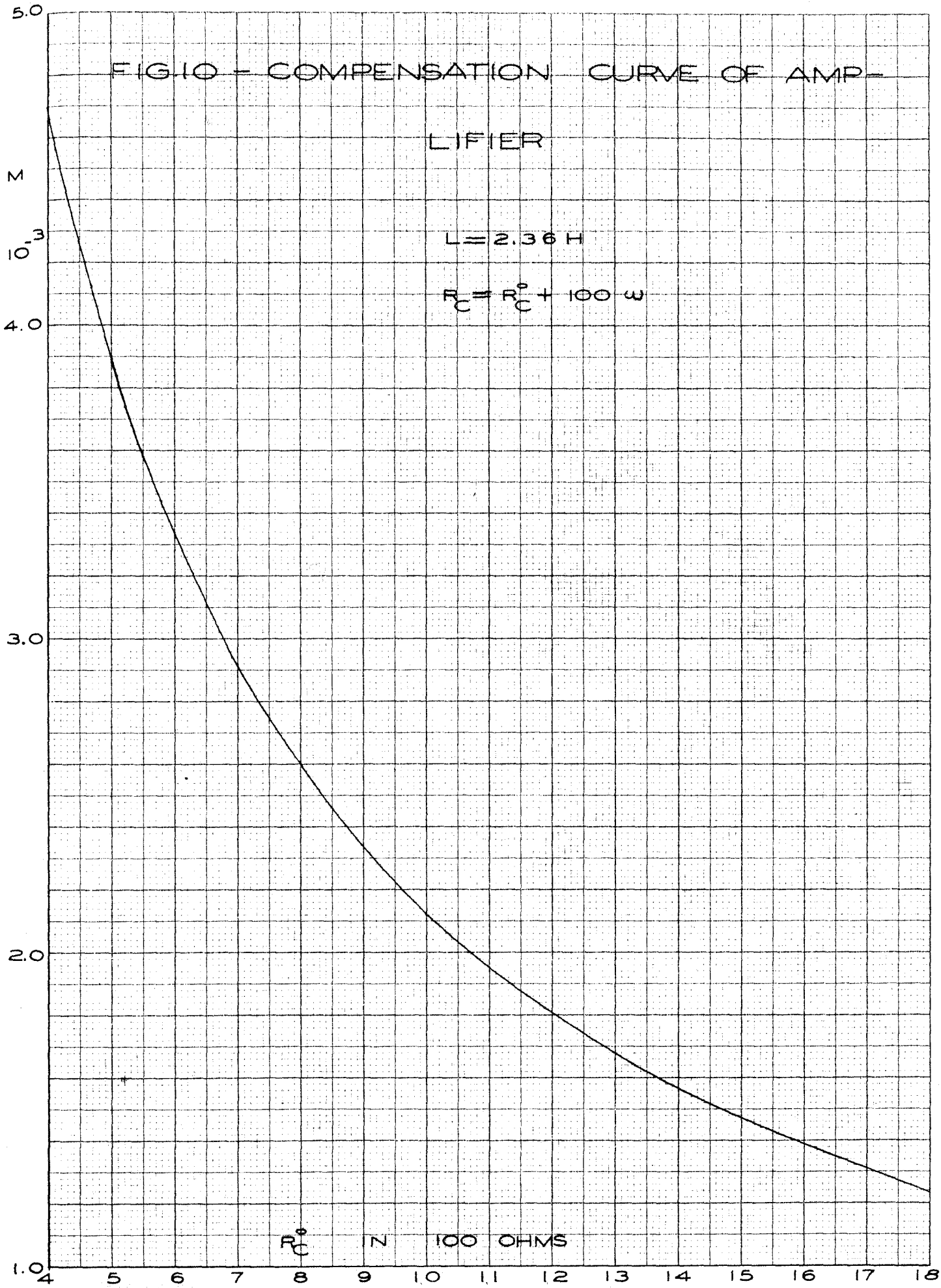
FIG.10 - COMPENSATION CURVE OF AMP-
LIFIER
L = 2.36 H
$R_C = R_C^o + 100\ \omega$
M
10^{-3}
5.0
4.0
3.0
2.0
1.0
4
5
6
7
8
9
10
11
12
13
14
15
16
17
18
R_C^o IN 100 OHMS

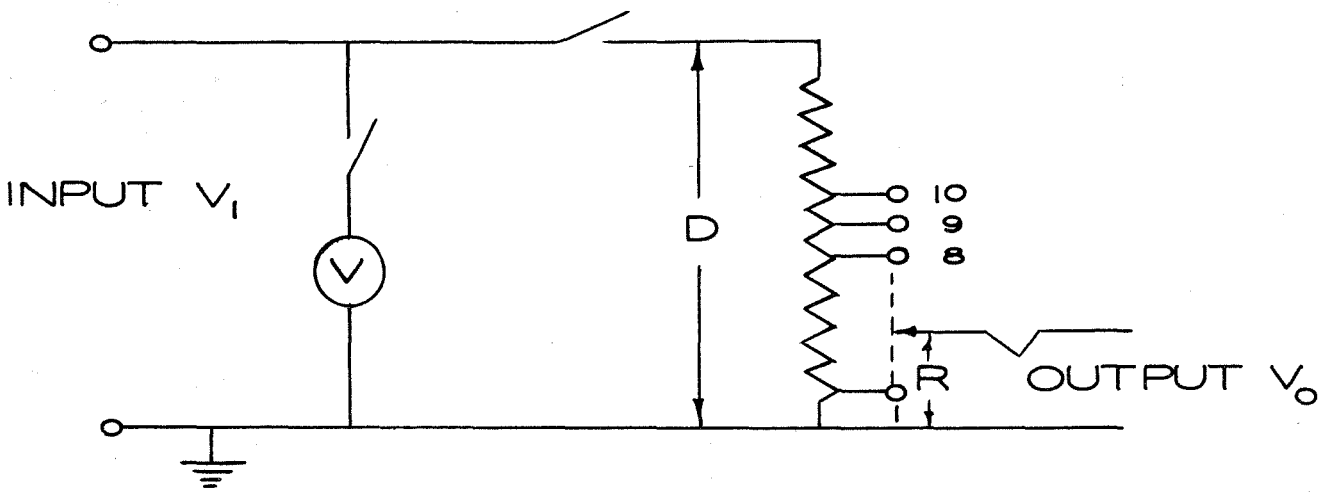

FIG. 11. VOLTAGE DIVIDER

TAP	R	R/D	D
1	0.000	0	5660
2	0.203	3.58×10^{-5}	
3	0.389	6.86×10^{-5}	
4	0.578	1.02×10^{-4}	
5	0.776	1.37×10^{-4}	
6	1.184	2.09×10^{-4}	
7	1.977	3.48×10^{-4}	
8	3.594	6.35×10^{-4}	
9	6.074	1.09×10^{-3}	
10	9.374	1.65×10^{-3}	

$$V_o = \frac{R}{D} V_I$$

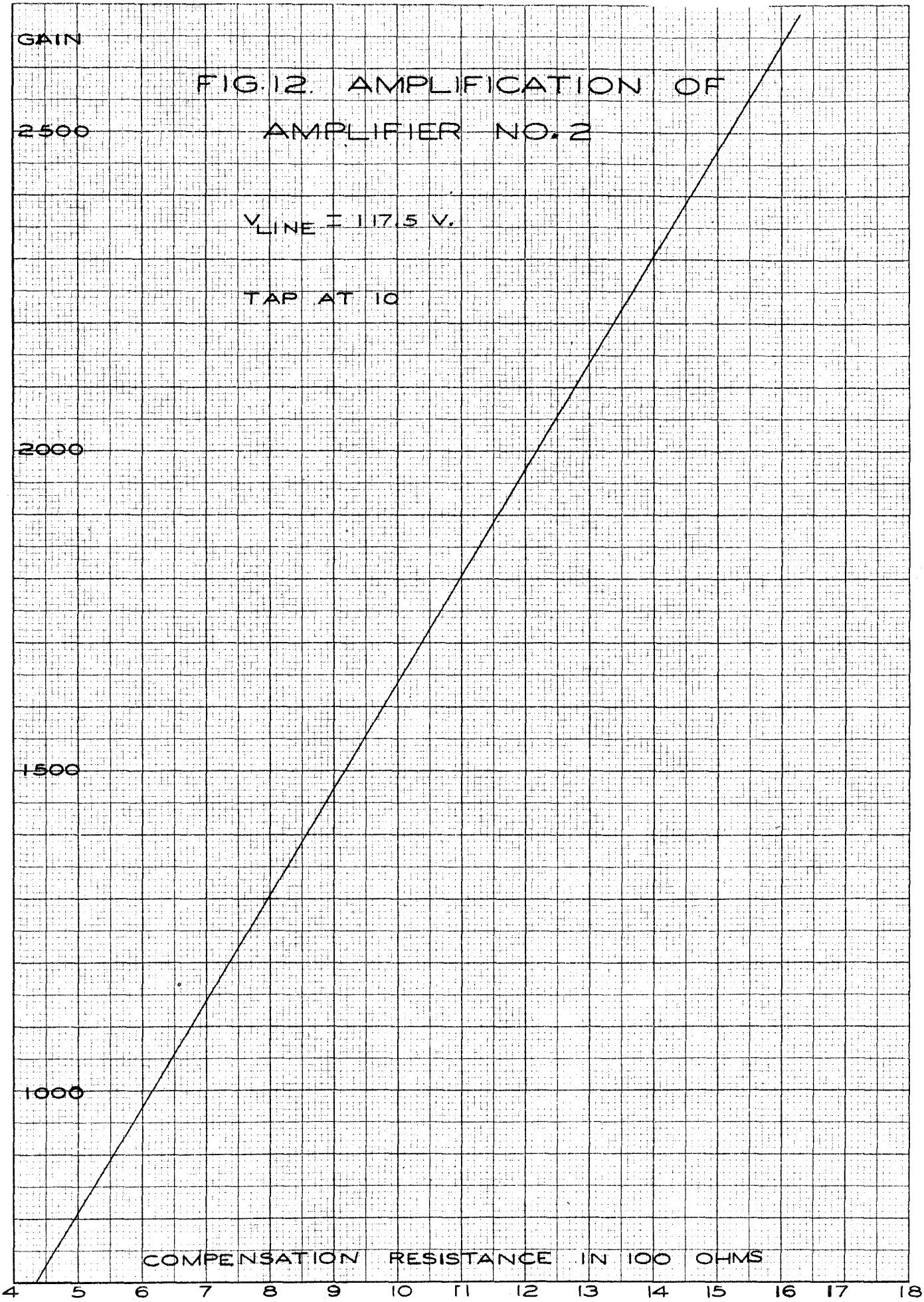

FIG. 12. AMPLIFICATION OF AMPLIFIER NO. 2

$V_{LINE} = 117.5$ V.

TAP AT 10

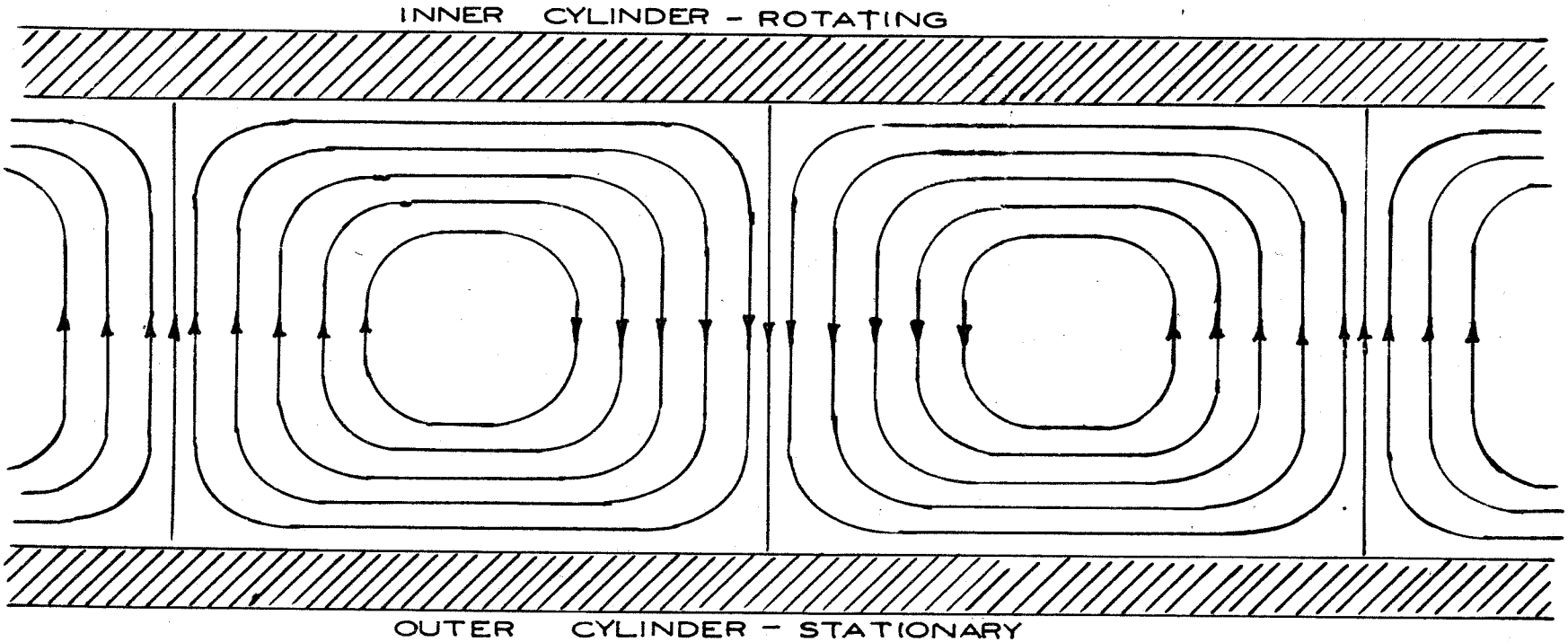

FIG. 13 - THE STREAMLINES OF RING-SHAPED VORTICES IN THE AXIAL PLANE OF ROTATING CYLINDERS

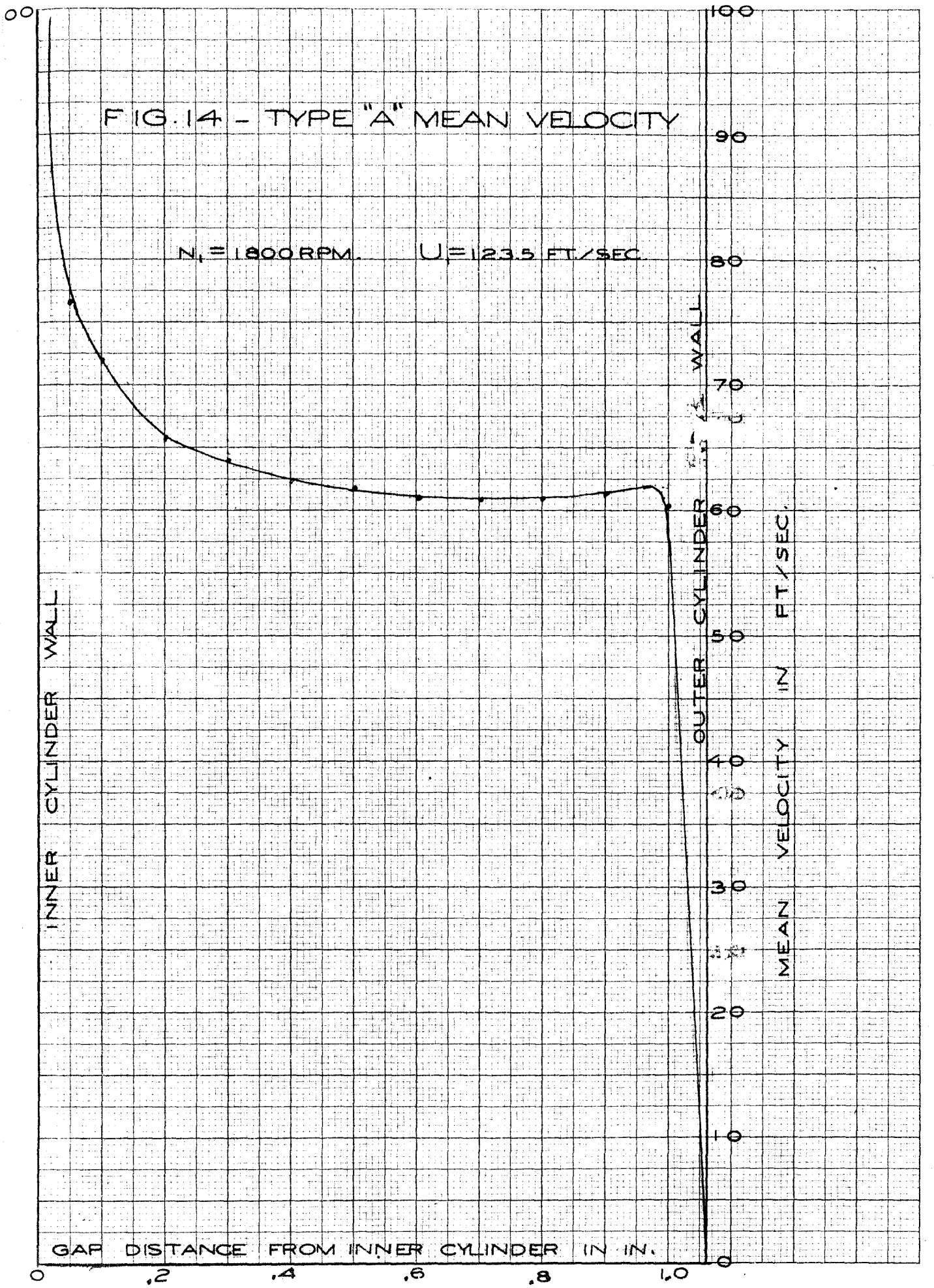
FIG. 14 - TYPE "A" MEAN VELOCITY
N₁ = 1800 RPM.
U₁ = 123.5 FT./SEC.
INNER CYLINDER WALL
OUTER CYLINDER WALL
MEAN VELOCITY IN FT/SEC.
GAP DISTANCE FROM INNER CYLINDER IN IN.
0
.2
.4
.6
.8
1.0
10
20
30
40
50
60
70
80
90
100

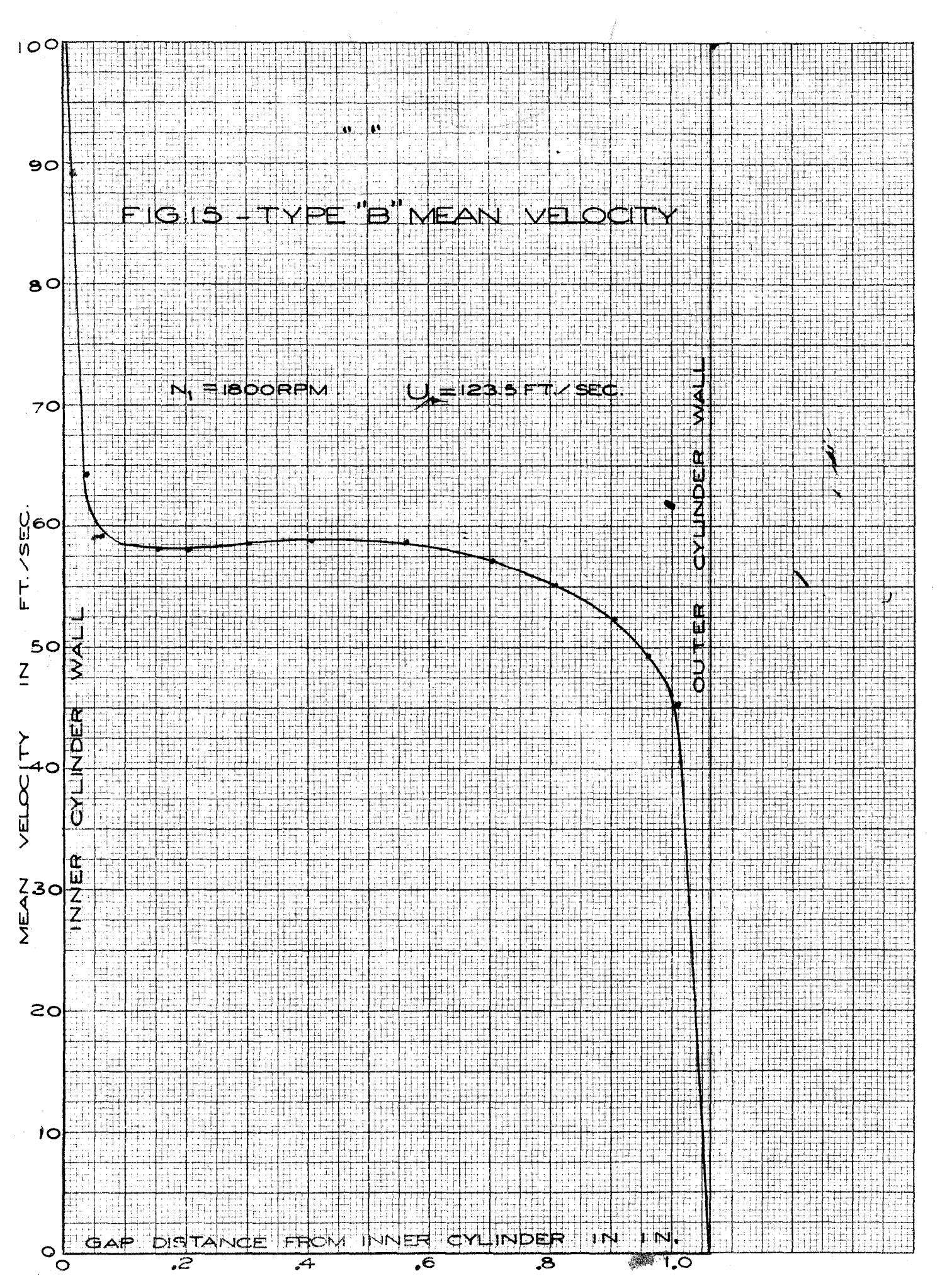
FIG.15 - TYPE "B" MEAN VELOCITY
N_1 = 1800 RPM.
U_1 = 123.5 FT./SEC.
MEAN VELOCITY IN FT./SEC.
INNER CYLINDER WALL
OUTER CYLINDER WALL
GAP DISTANCE FROM INNER CYLINDER IN IN.
0
10
20
30
40
50
60
70
80
90
100
.2
.4
.6
.8
1.0

FIG.16-TYPE "A" TURBULENCE DISTRIBUTION

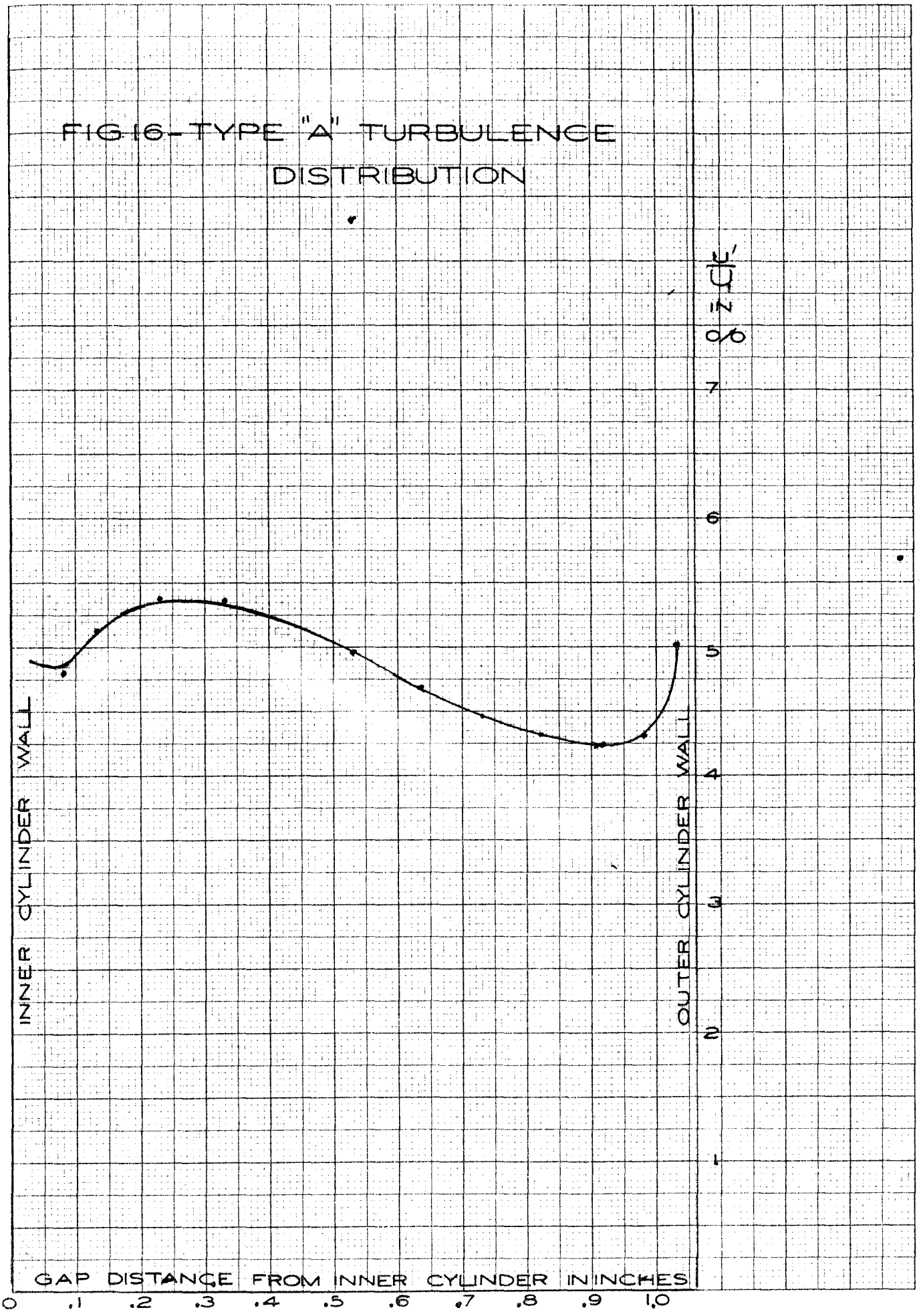

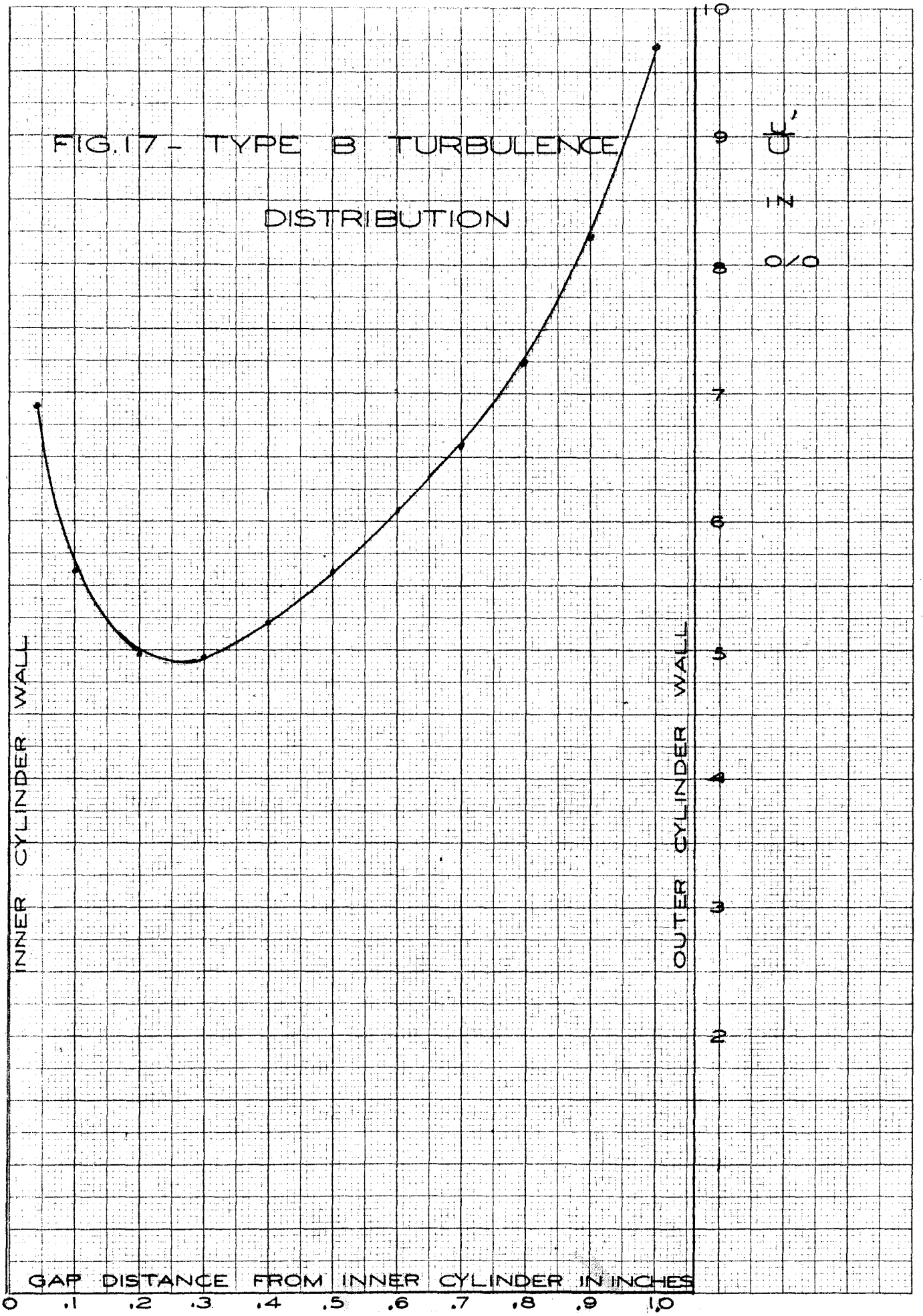
FIG. 17 - TYPE B TURBULENCE DISTRIBUTION
INNER CYLINDER WALL
OUTER CYLINDER WALL
GAP DISTANCE FROM INNER CYLINDER IN INCHES
0
.1
.2
.3
.4
.5
.6
.7
.8
.9
1.0
2
3
4
5
6
7
8
9
10
$\frac{u'}{U}$ IN %

FIG. 18. — MEAN VELOCITY DISTRIBUTION SHOWING TRANSITION OF FLOW PATTERN

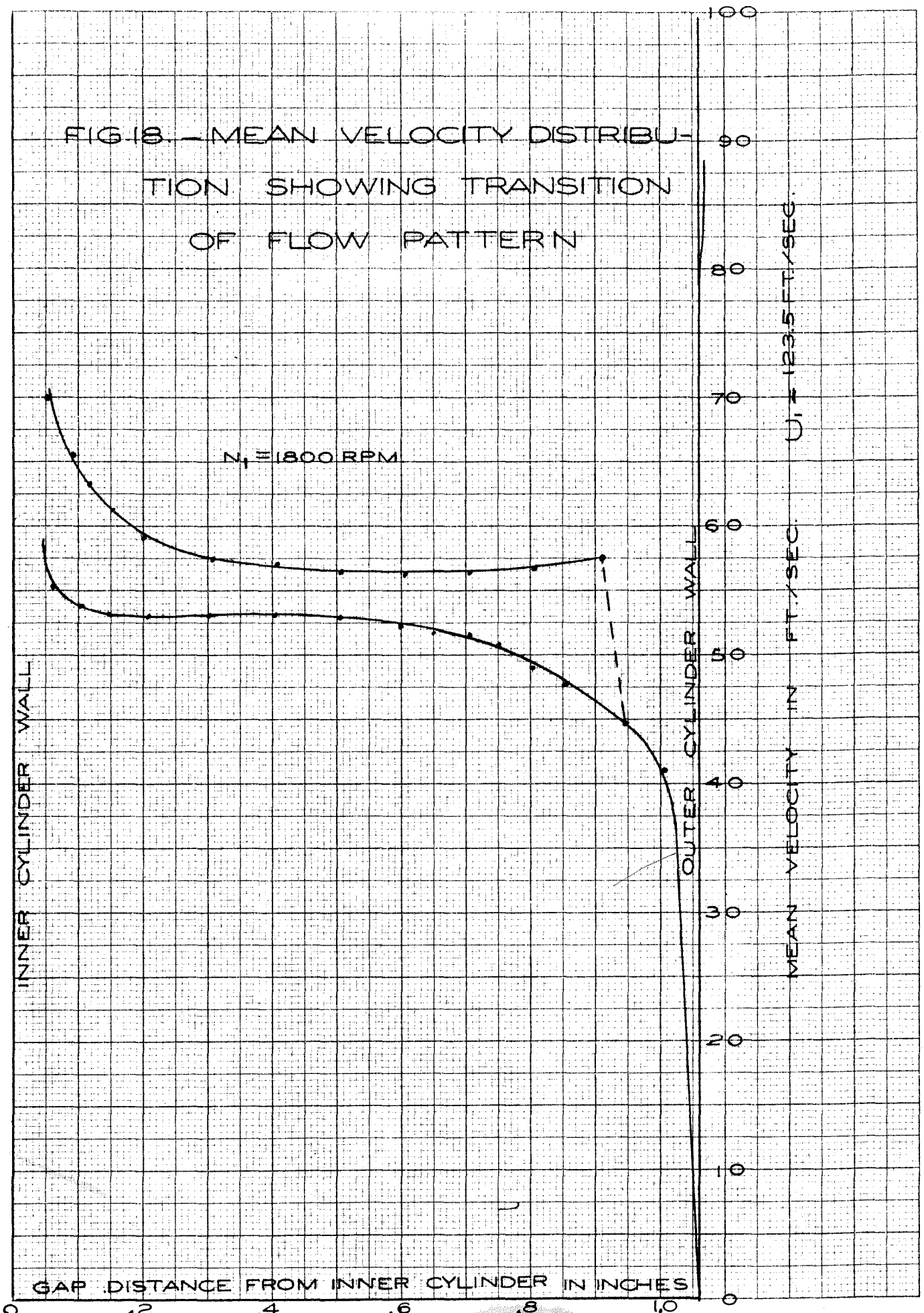

FIG 19 - MEAN VELOCITY DISTRIBUTION WITH DUMMY HOT-WIRE

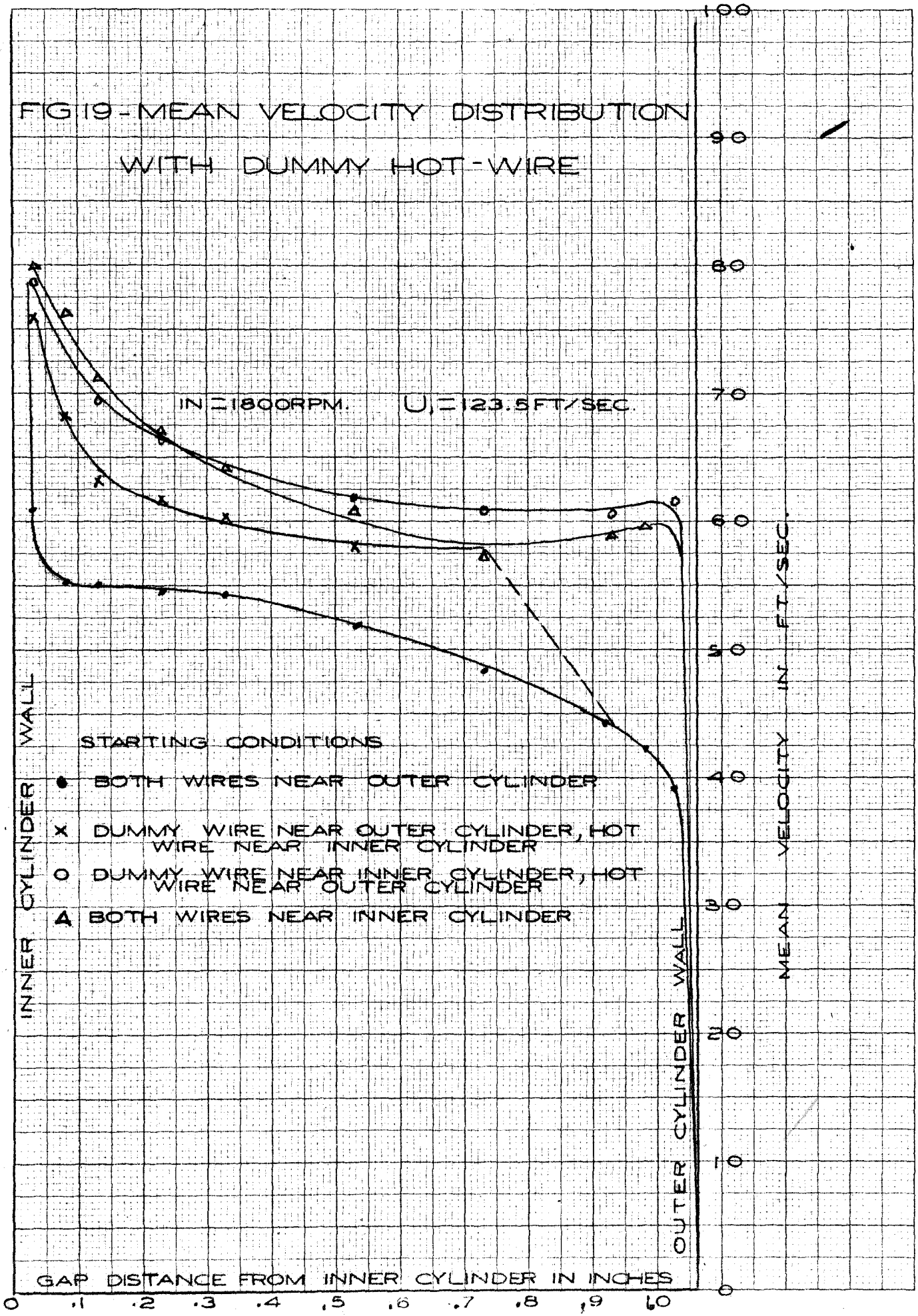

FIG. 20 - STATIC PRESSURE DISTRIBUTION WITH ENDS OF CYLINDERS TIGHTLY CLOSED (SEE FIG 1-A)

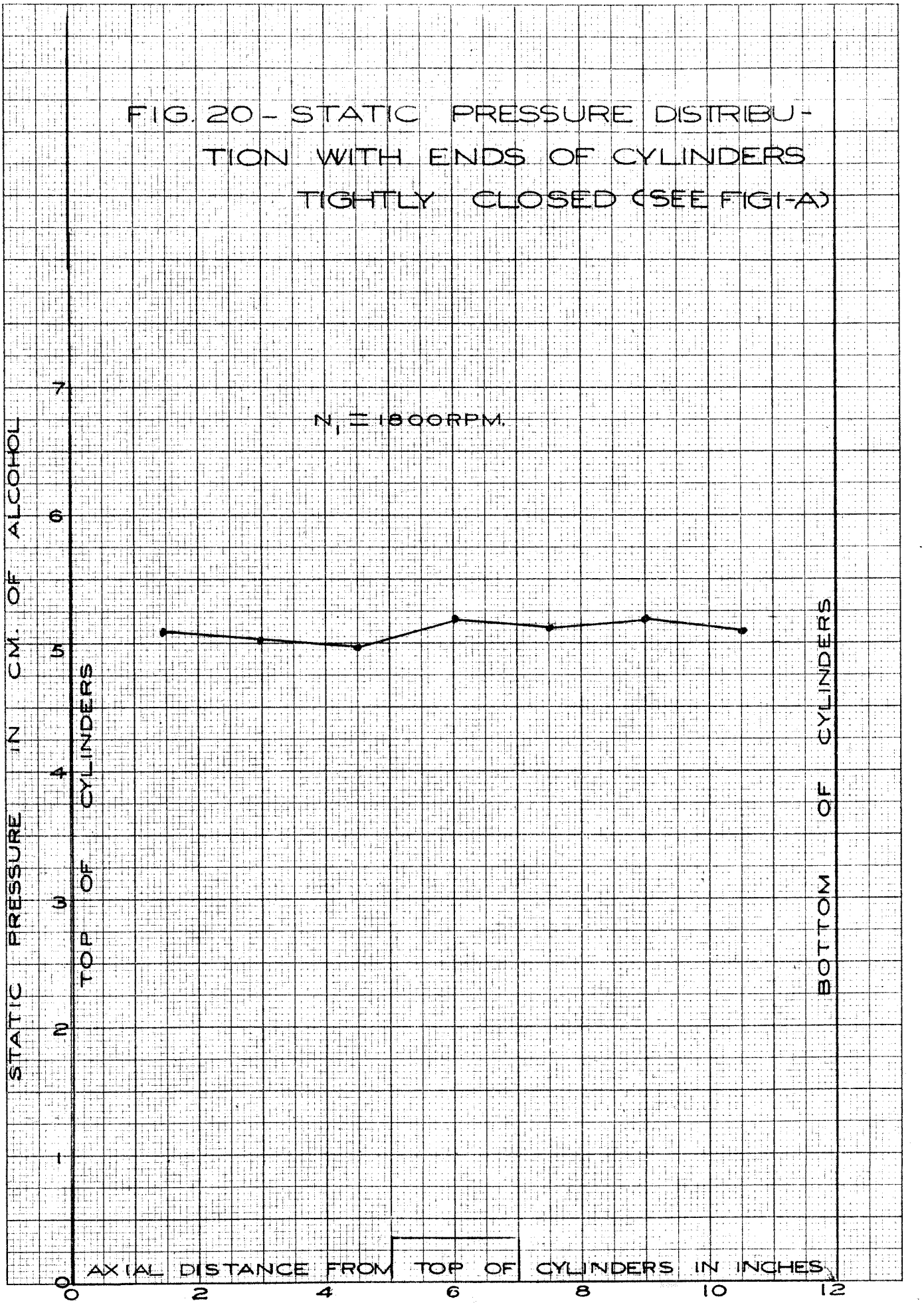

FIG. 21 - STATIC PRESSURE DISTRIBUTION WITH ENDS OF CYLINDERS SHOWN AS IN FIG. 1-C

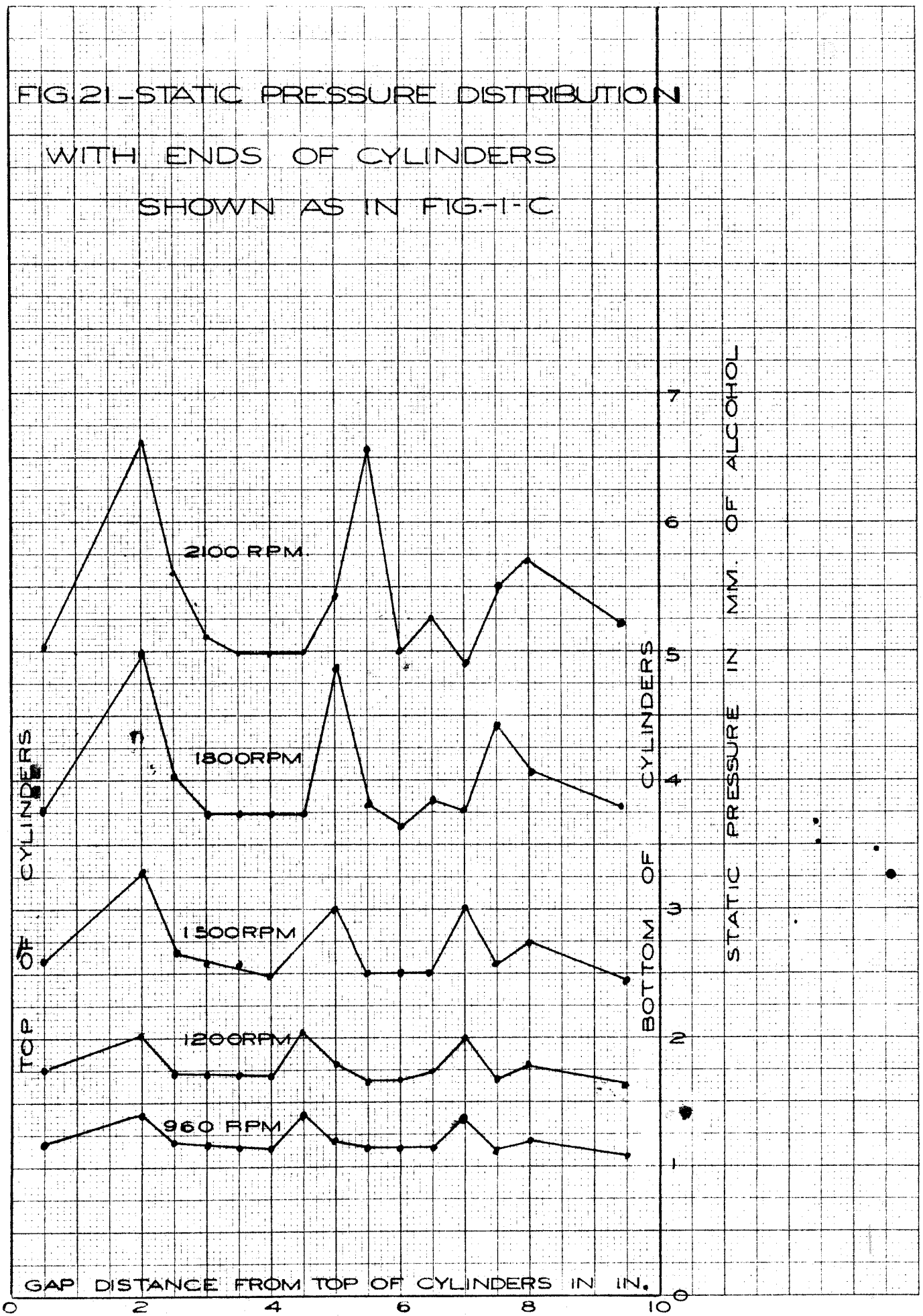

FIG. 22 - MEAN VELOCITY DISTRIBUTION AT N_1 = 1200 RPM

MEAN VELOCITY DIAGRAMS

STATION NO.1
TYPE B

STATION NO.2
TYPE A

STATION NO.3
TYPE A

STATION NO.4
TPYE A_B

STATION NO.5
TYPE B

STATION NO.6
TYPE B

STATION NO.7
TYPE A_B

MEAN VELOCITY - SOLID CURVES - IN FT./SEC.
U_1 = 82.4 FT/SEC.

INNER CYLINDER WALL

45
40
35

GAP DISTANCE FROM INNER CYLINDER IN INCHES

0 .1 .2 .3 .4 .5

DOTTED CURVES - AVERAGE MEAN VELOCITY CURVE

OUTER CYLINDER WALL

STATIC PRESSURE DISTRIBUTIONS

STATIC PRESSURE IN MM. OF ALCOHOL

2.0
1.0

1 2 3 4 5 6 7

TOP OF CYLINDERS

BOTTOM OF CYLINDERS

0 2 4 6 8 10

AXIAL DISTANCE FROM TOP OF CYLINDERS IN INCHES

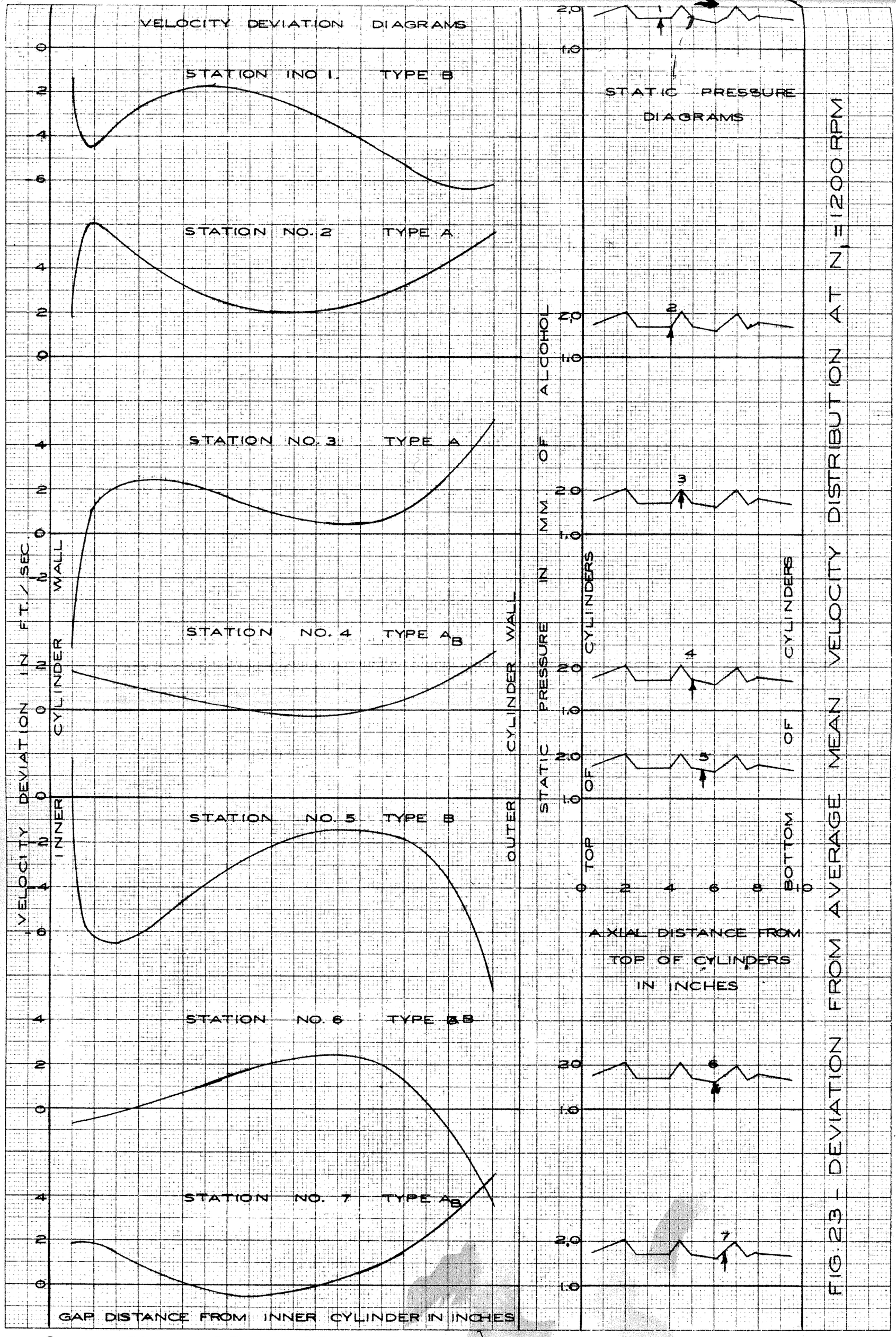

FIG. 23 - DEVIATION FROM AVERAGE MEAN VELOCITY DISTRIBUTION AT N = 1200 RPM

FIG. 24 - TURBULENCE DISTRIBUTION AT N_1 = 1,200 RPM

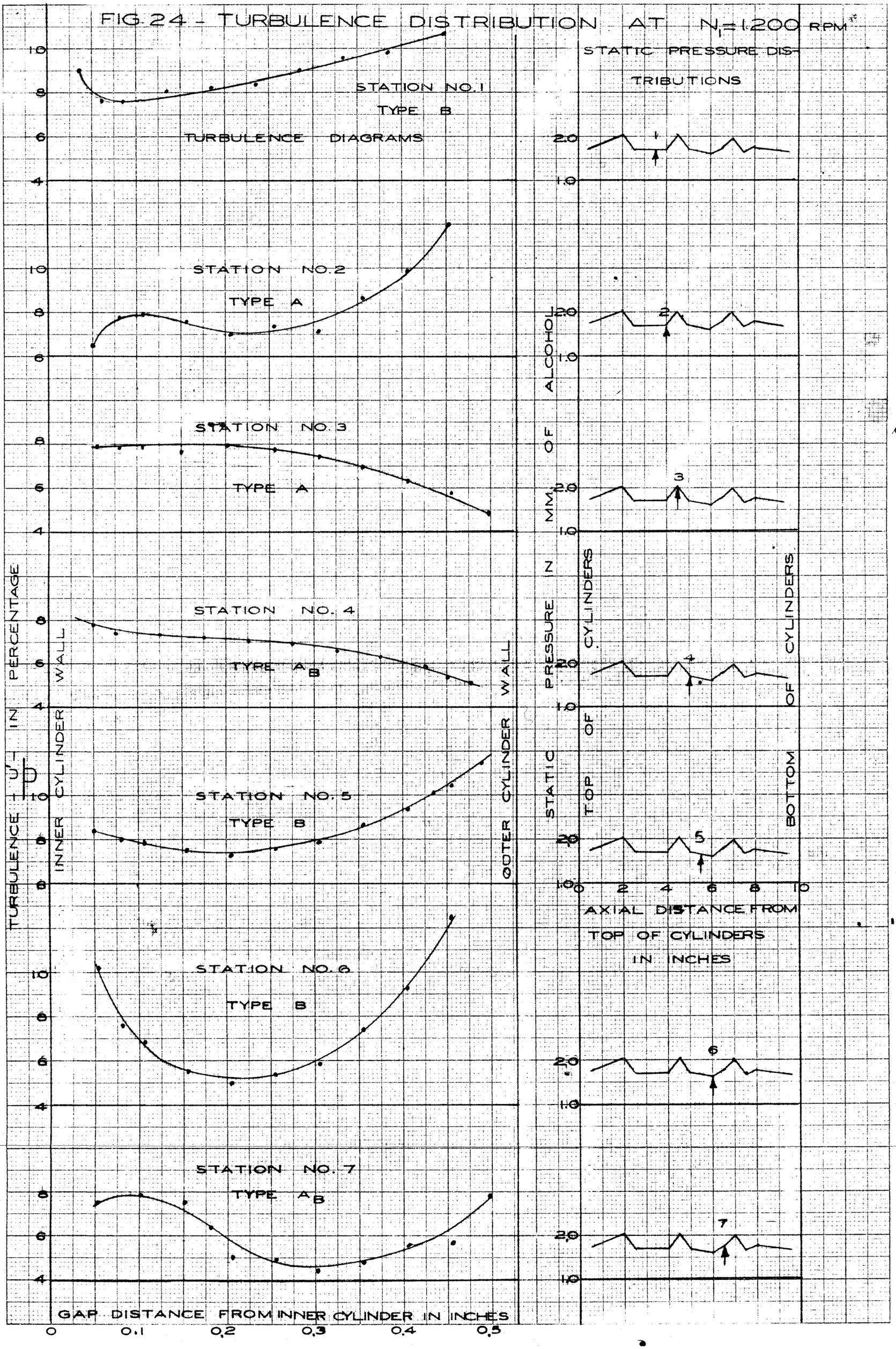

FIG. 25 – MEAN VELOCITY DISTRIBUTION AT $N_1 = 960$ RPM

MEAN VELOCITY DIAGRAMS

$U_1 = 65.8$ FT./SEC.

MEAN VELOCITY – FULL-LINE CURVES – IN FT/SEC.

STATION NO. 1 TYPE B

STATION NO. 2 TYPE A

STATION NO. 3 TYPE A

STATION NO. 4 TYPE AB

STATION NO. 5 TYPE B

STATION NO. 6 TYPE B

STATION NO. 7 TYPE AB

INNER CYLINDER WALL

OUTER CYLINDER WALL

DOTTED CURVES – AVERAGE MEAN VELOCITY CURVE

GAP DISTANCE FROM INNER CYLINDER IN INCHES

STATIC PRESSURE DIAGRAMS

STATIC PRESSURE IN MM OF ALCOHOL

TOP OF CYLINDERS

BOTTOM OF CYLINDERS

AXIAL DISTANCE FROM TOP OF CYLINDERS IN INCHES

VELOCITY DEVIATION DIAGRAMS

STATION NO.1 TYPE B

STATION NO.2 TYPE A

STATION NO.3 TYPE A

STATION NO 4 TYPE A

STATION NO.5 TYPE B

STATION NO.6 TYPE B

STATION NO 7 TYPE A

VELOCITY DEVIATION U — IN FT./SEC.

INNER CYLINDER WALL

OUTER CYLINDER WALL

GAP DISTANCE FROM INNER CYLINDER IN INCHES

STATIC PRESSURE DIAGRAMS

STATIC PRESSURE IN MM. OF ALCOHOL

TOP OF CYLINDERS

BOTTOM OF CYLINDERS

AXIAL DISTANCE FROM TOP OF CYLINDERS IN INCHES

FIG. 26 - DEVIATION FROM AVERAGE MEAN VELOCITY DISTRIBUTION AT N_1 = 960 RPM.

FIG. 27 — TURBULENCE DISTRIBUTION AT N = 960 RPM.

TURBULENCE DIAGRAMS

STATION NO. 1 TYPE B

STATION NO. 2 TYPE A

STATION NO. 3 TYPE A

STATION NO. 4 TYPE A B

STATION NO. 5 TYPE B

STATION NO. 6 TYPE B

STATION NO. 7 TYPE A

MEAN TURBULENCE U'/U IN OUTER CYLINDER WALL / INNER CYLINDER WALL

GAP DISTANCE FROM INNER CYLINDER IN IN.

STATIC PRESSURE DIAGRAMS

STATIC PRESSURE IN MM. OF ALCOHOL

TOP OF CYLINDERS

BOTTOM OF CYLINDERS

AXIAL DISTANCE FROM TOP OF CYLINDERS IN INCHES

FIG. 28 - MEAN VELOCITY DISTRIBUTION AT N_1 = 150 RPM.

MEAN VELOCITY DIAGRAMS

U_1 = 103.5 FT/SEC.

MEAN VELOCITY - FULL-LINE CURVES - IN FT./SEC.

STATION NO. 1 TYPE B

STATION NO. 2 TYPE A

STATION NO. 3 TYPE A

STATION NO. 4 TYPE AB

STATION NO. 5 TYPE B

STATION NO. 6 TYPE B

STATION NO. 7 TYPE AB

INNER CYLINDER WALL

OUTER CYLINDER WALL

DOTTED - CURVES - AVERAGE MEAN VELOCITY CURVE

GAP DISTANCE FROM INNER CYLINDER IN IN.

0 1 2 3 4 5

45 50 55

STATIC PRESSURE DIAGRAMS

STATIC PRESSURE IN MM. OF ALCOHOL

2.0 3.0

TOP OF CYLINDERS

BOTTOM OF CYLINDERS

1 2 3 4 5 6 7

AXIAL DISTANCE FROM TOP OF CYLINDERS IN INCHES

0 2 4 6 8 10

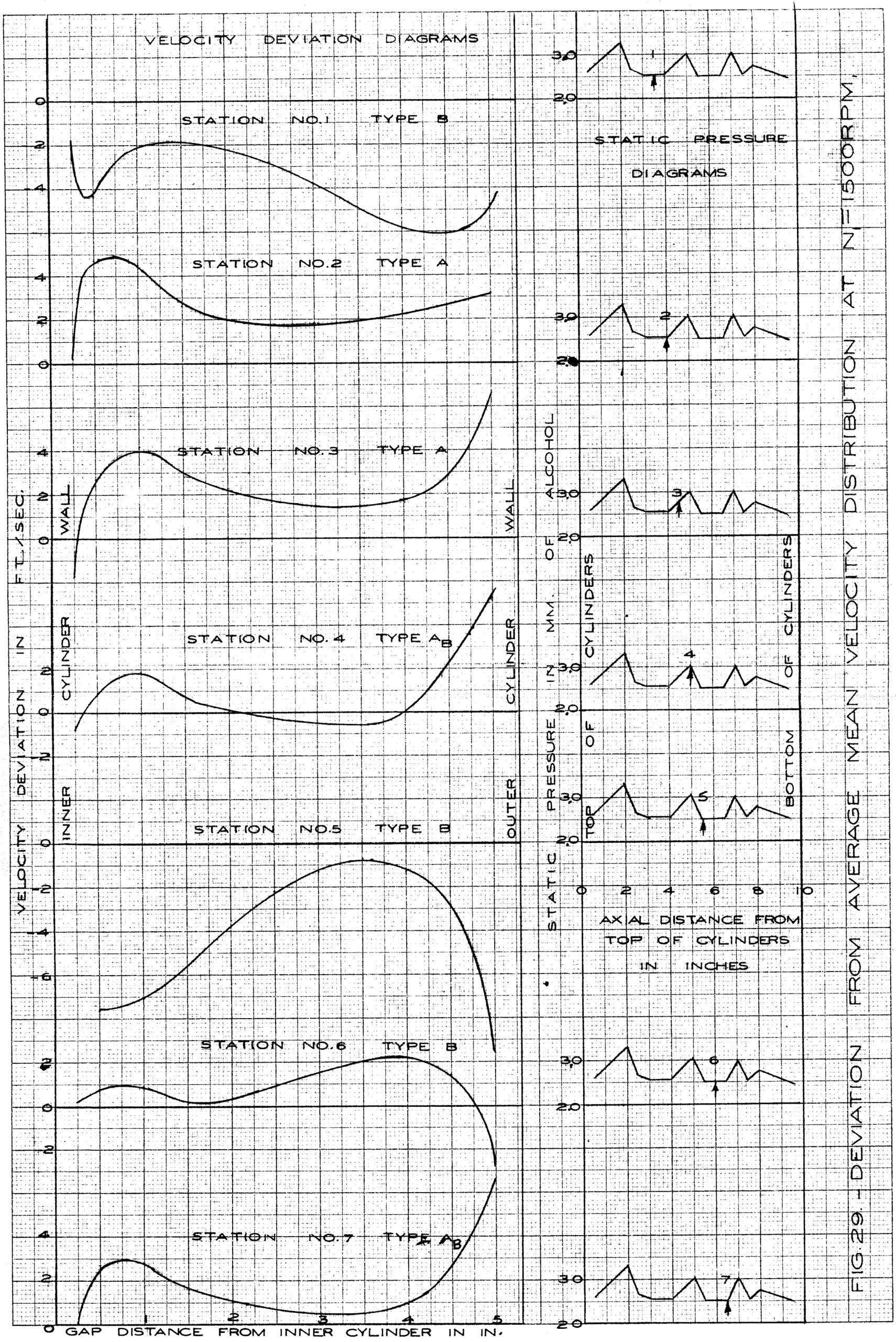

FIG. 29. DEVIATION FROM AVERAGE MEAN VELOCITY DISTRIBUTION AT N=1500 R.P.M.

FIG. 30 – TURBULENCE DISTRIBUTION AT N_1 = 1500 RPM

TURBULENCE DIAGRAMS

STATIC PRESSURE DIAGRAMS

STATION NO. 1 TYPE B

STATION NO. 2 TYPE A

STATION NO. 3 TYPE A

STATION NO. 4 TYPE A_B

STATION NO. 5 TYPE B

STATION NO. 6 TYPE B

STATION NO. 7 TYPE A_B

TURBULENCE U/U PERCENTAGE

WALL

CYLINDER

INNER

OUTER

GAP DISTANCE FROM INNER CYLINDER IN IN.

MM. ALCOHOL

STATIC PRESSURE IN CYLINDERS

TOP OF CYLINDERS

BOTTOM OF CYLINDERS

AXIAL DISTANCE FROM TOP OF CYLINDERS IN INCHES

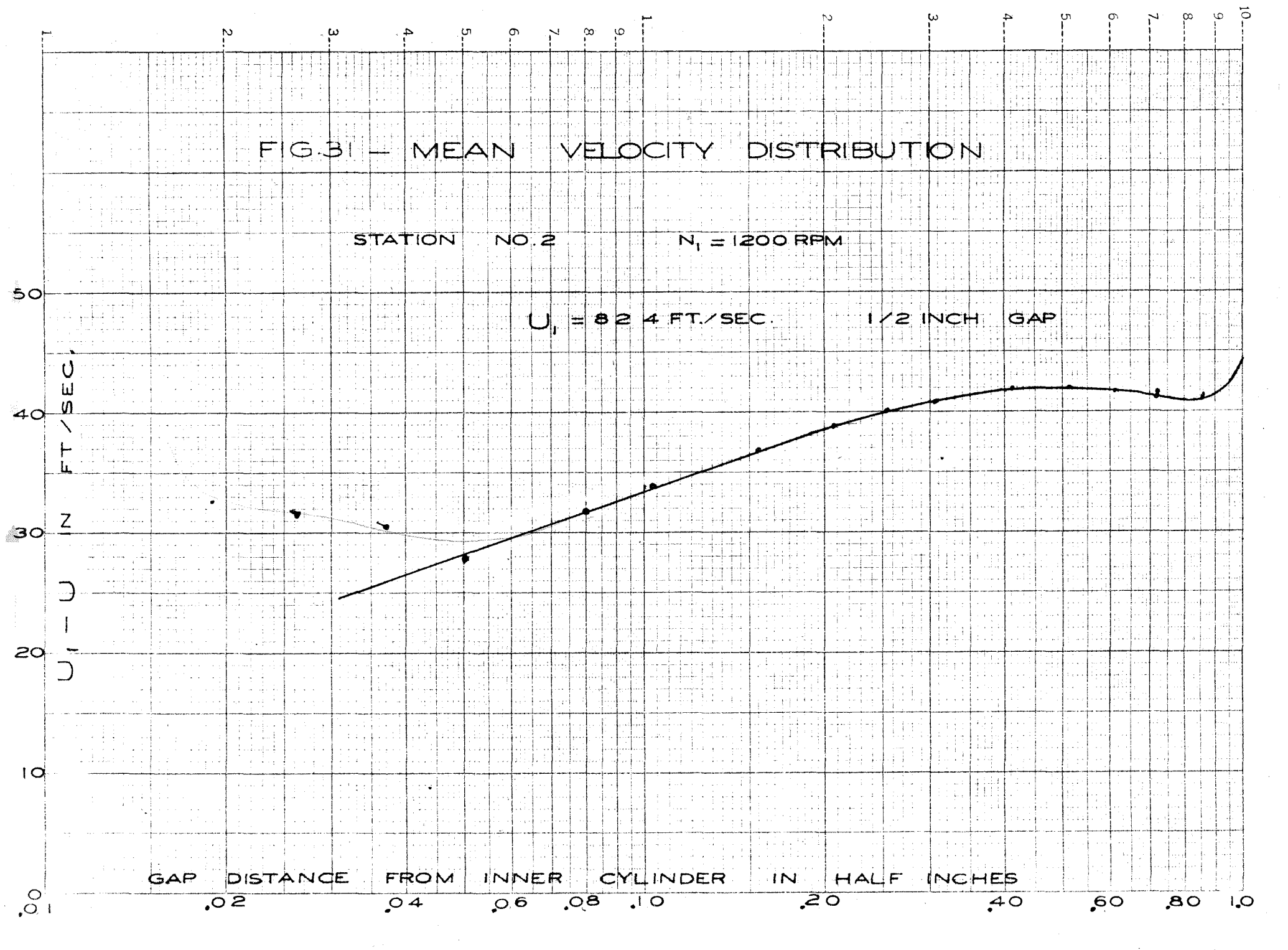
FIG.31 – MEAN VELOCITY DISTRIBUTION
STATION NO. 2
N_1 = 1200 RPM
U_1 = 82.4 FT./SEC.
1/2 INCH GAP
$U_1 - U$ IN FT/SEC.
50
40
30
20
10
0.0
GAP DISTANCE FROM INNER CYLINDER IN HALF INCHES
.02
.04
.06
.08
.10
.20
.40
.60
.80
1.0

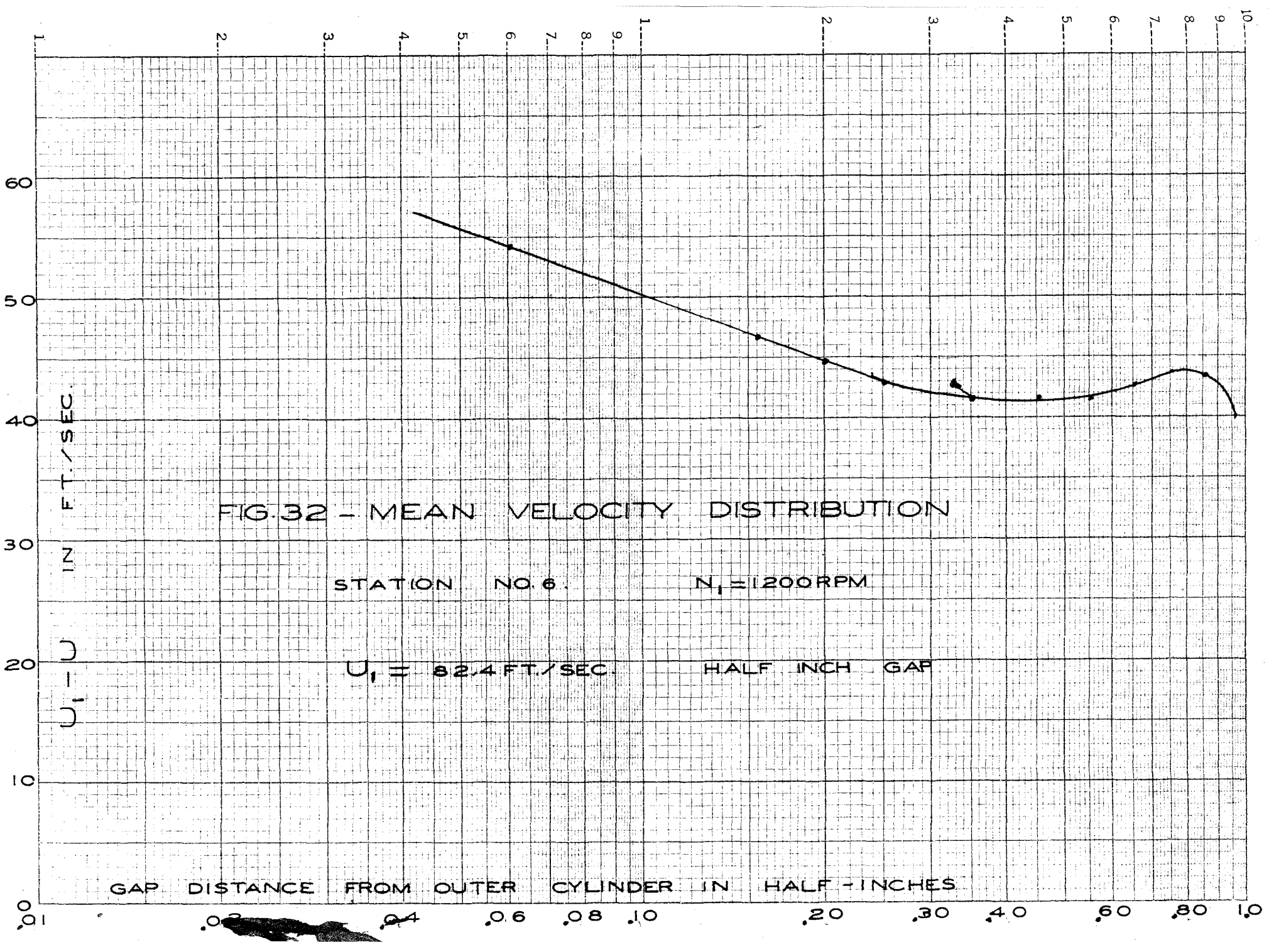
$U_1 - U$ IN FT./SEC.
0
10
20
30
40
50
60
GAP DISTANCE FROM OUTER CYLINDER IN HALF-INCHES
.01
.02
.04
.06
.08
.10
.20
.30
.40
.60
.80
1.0
FIG. 32 - MEAN VELOCITY DISTRIBUTION
STATION NO. 6.
N_1 = 1200 RPM
U_1 = 82.4 FT./SEC.
HALF INCH GAP

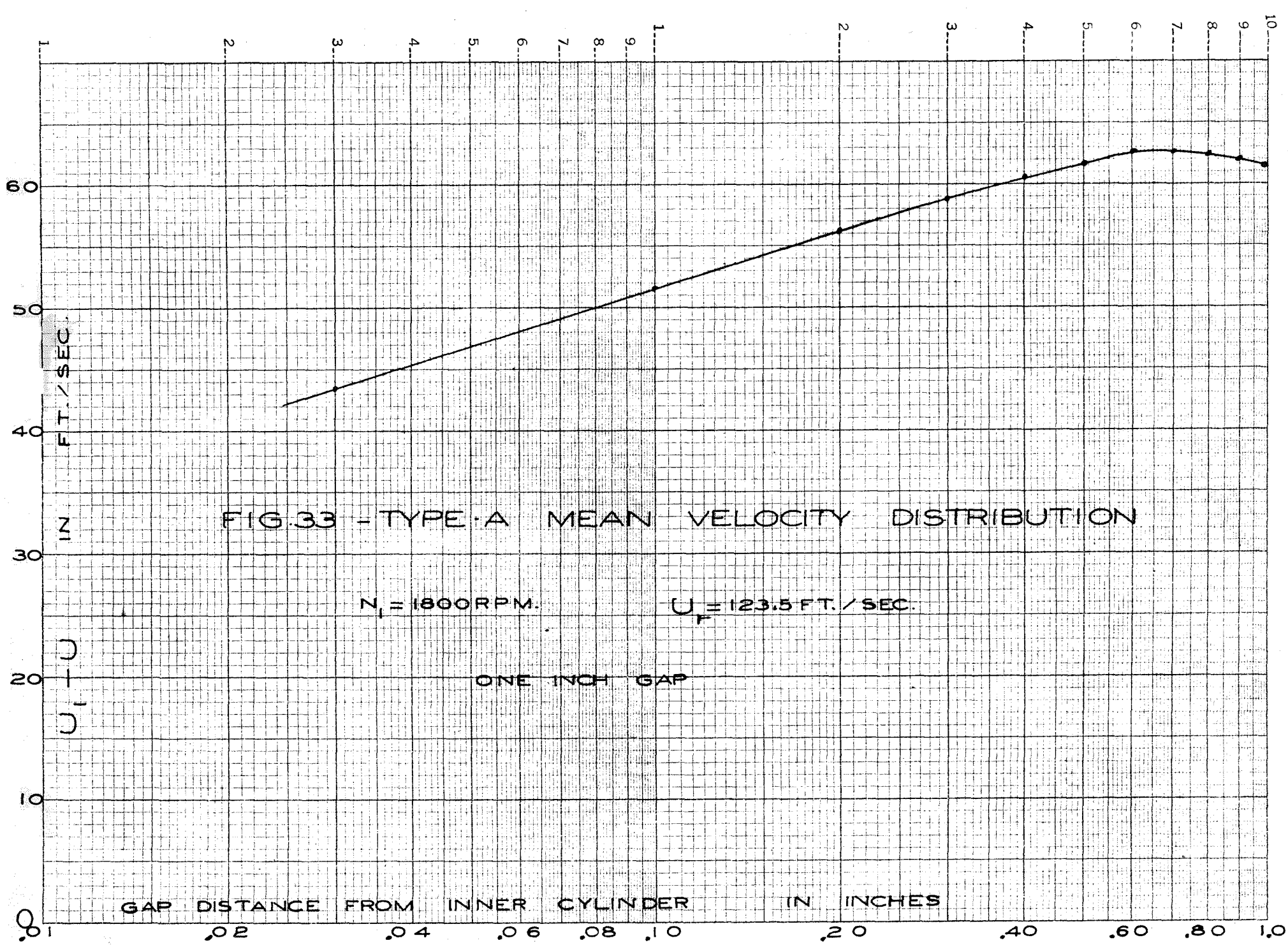
FIG.33 - TYPE-A MEAN VELOCITY DISTRIBUTION
N_1 = 1800 R.P.M.
U_F = 123.5 FT./SEC.
ONE INCH GAP
U_1 IN FT./SEC.
GAP DISTANCE FROM INNER CYLINDER IN INCHES
0
10
20
30
40
50
60
.01
.02
.04
.06
.08
.10
.20
.40
.60
.80
1.0

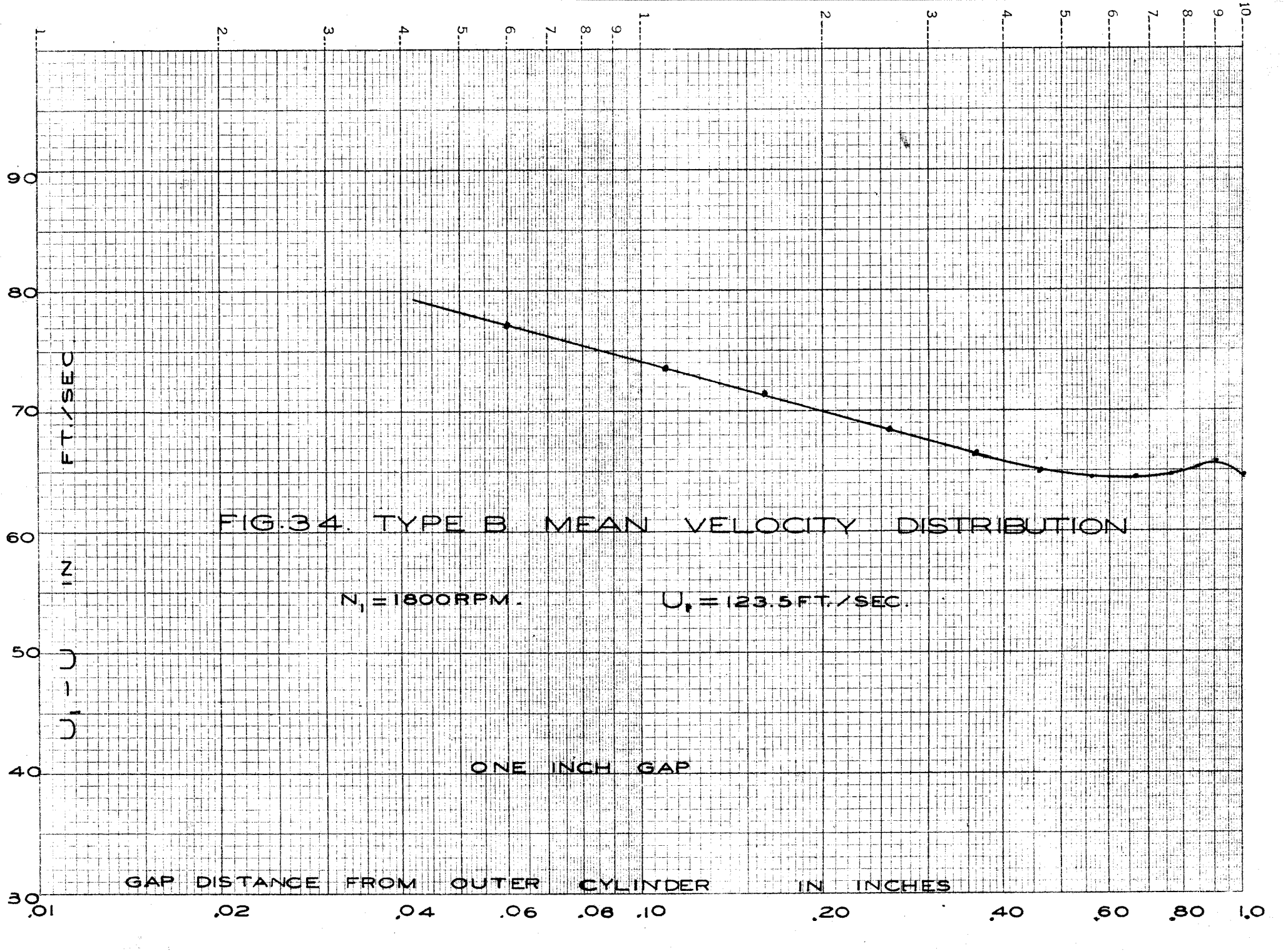

FIG. 34. TYPE B MEAN VELOCITY DISTRIBUTION

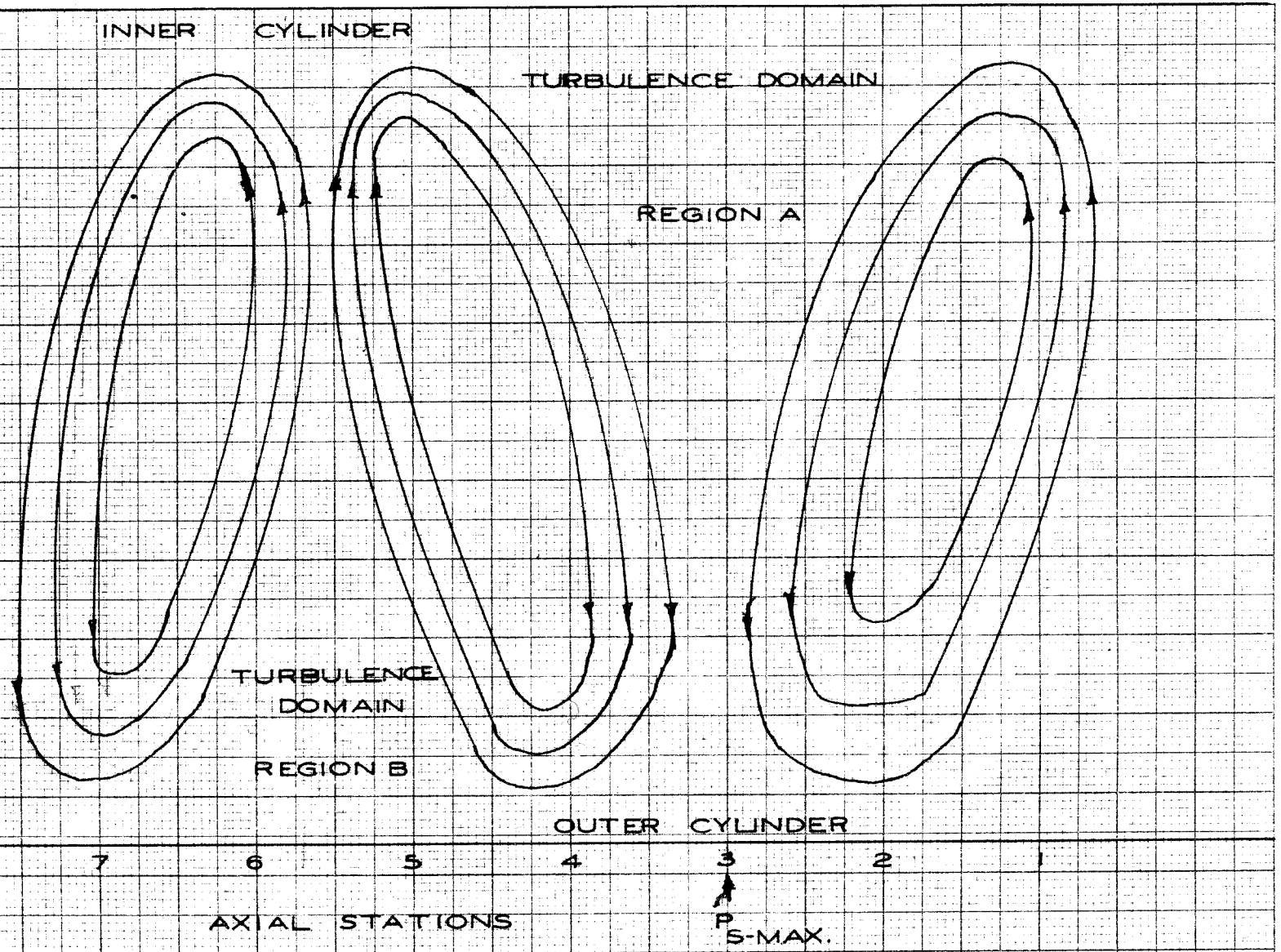

FIG 35. VORTICES IN OUR CYLINDERS

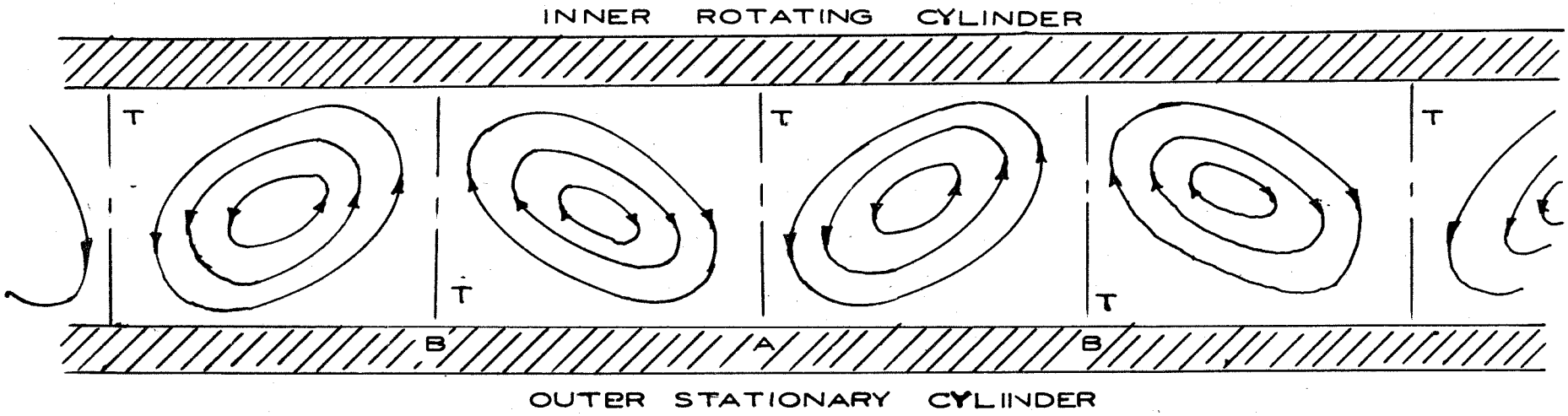

FIG. 36 VORTICES IN OUR CYLINDERS

T = TURBULENCE DOMAIN

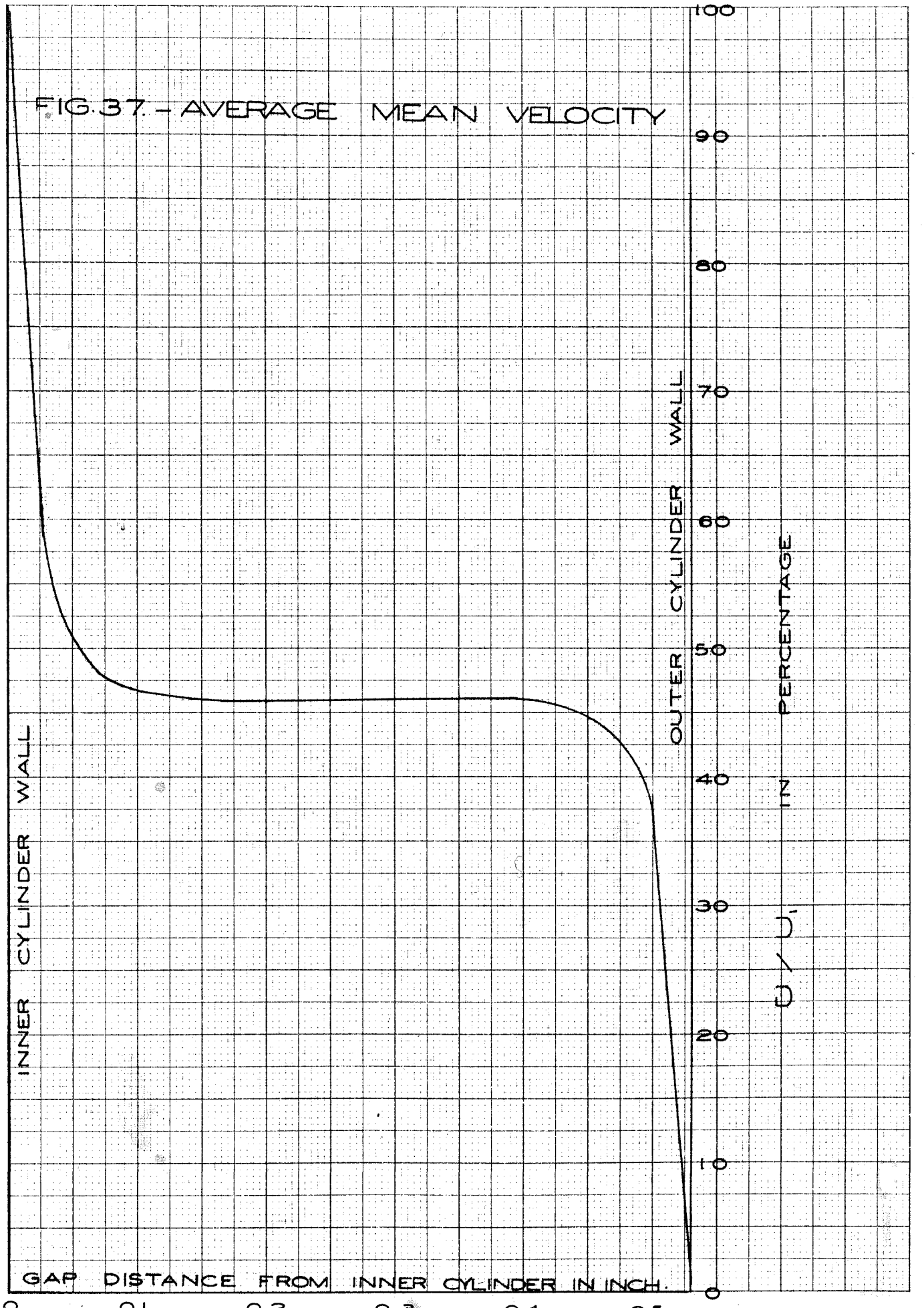
FIG. 37. - AVERAGE MEAN VELOCITY
INNER CYLINDER WALL
OUTER CYLINDER WALL
U / U1 IN PERCENTAGE
100
90
80
70
60
50
40
30
20
10
0
GAP DISTANCE FROM INNER CYLINDER IN INCH.
0
0,1
0,2
0,3
0,4
0,5

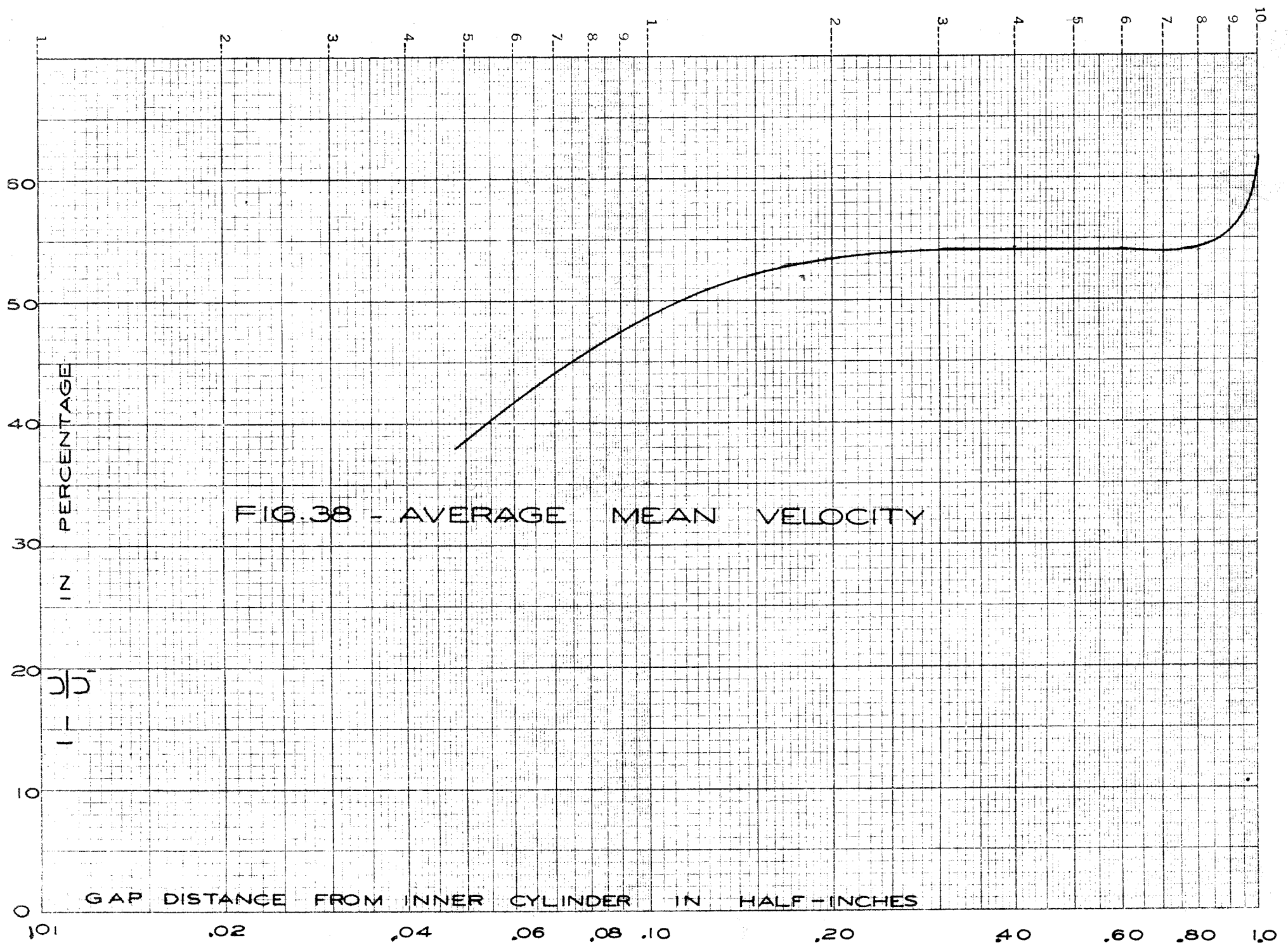

FIG. 38 - AVERAGE MEAN VELOCITY

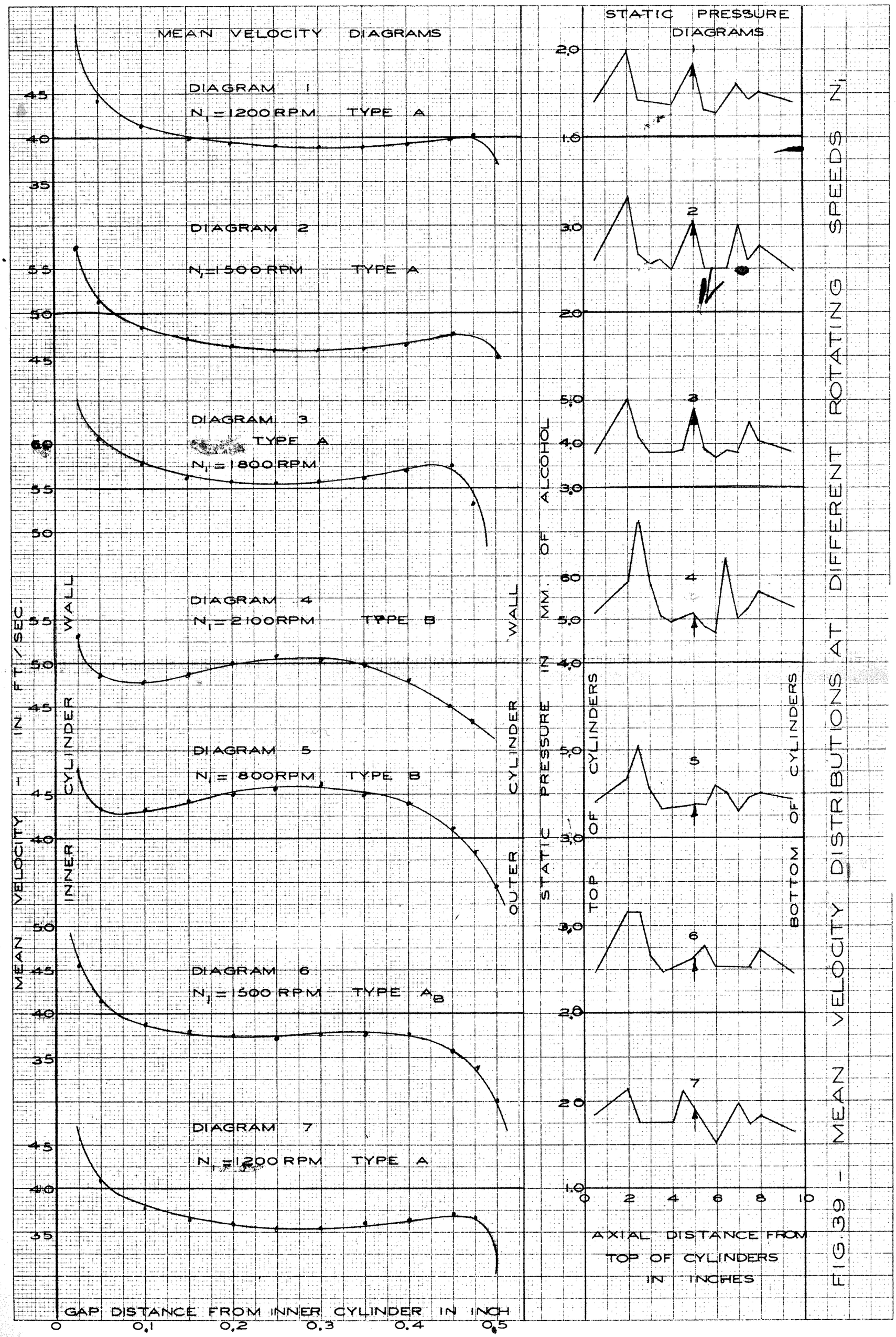

FIG. 39 - MEAN VELOCITY DISTRIBUTIONS AT DIFFERENT ROTATING SPEEDS N_1

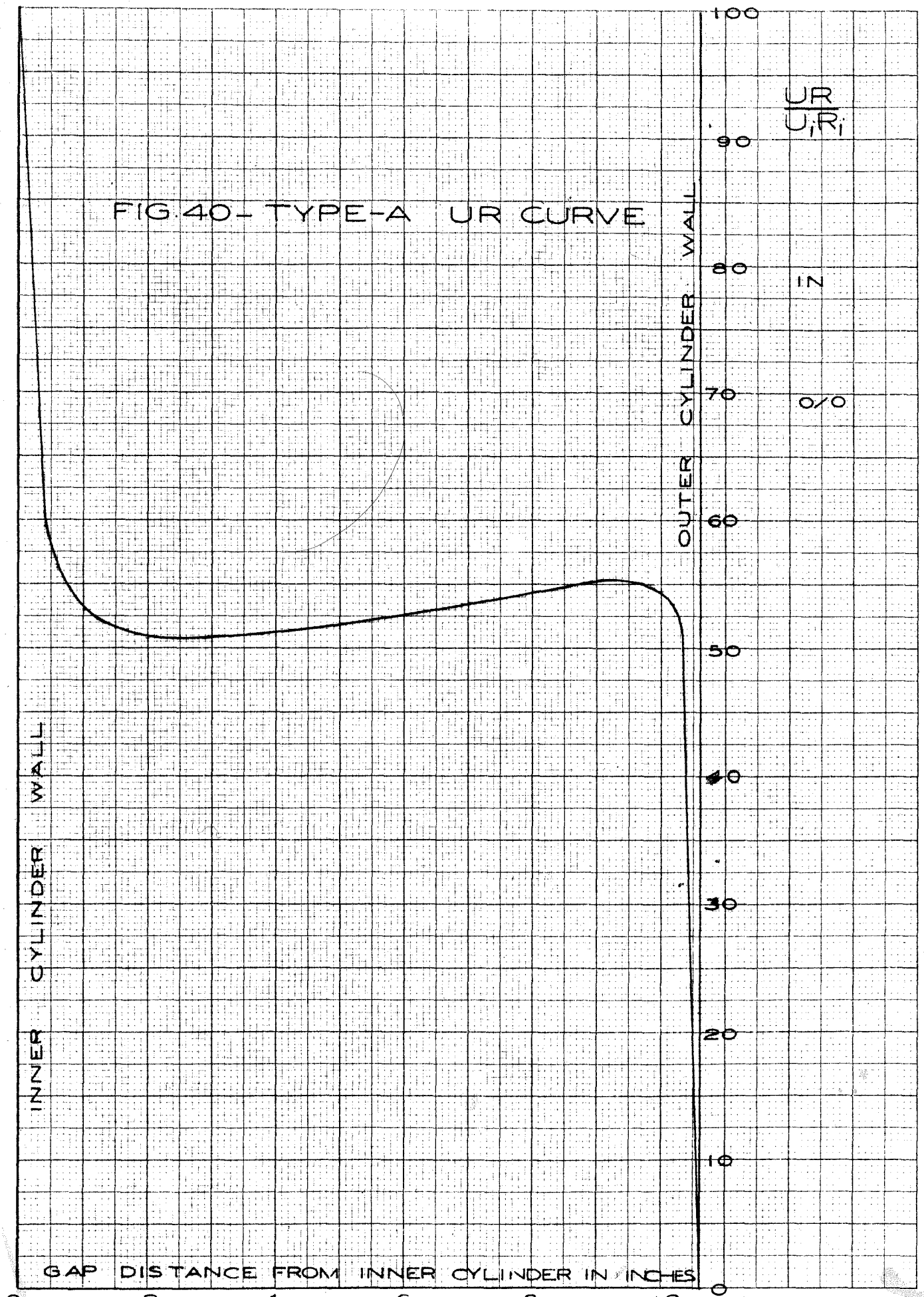
FIG.40- TYPE-A UR CURVE
UR / U₁R₁
100
90
80
70
60
50
40
30
20
10
0
IN
0/0
OUTER CYLINDER WALL
INNER CYLINDER WALL
GAP DISTANCE FROM INNER CYLINDER IN INCHES
0
.2
.4
.6
.8
1.0

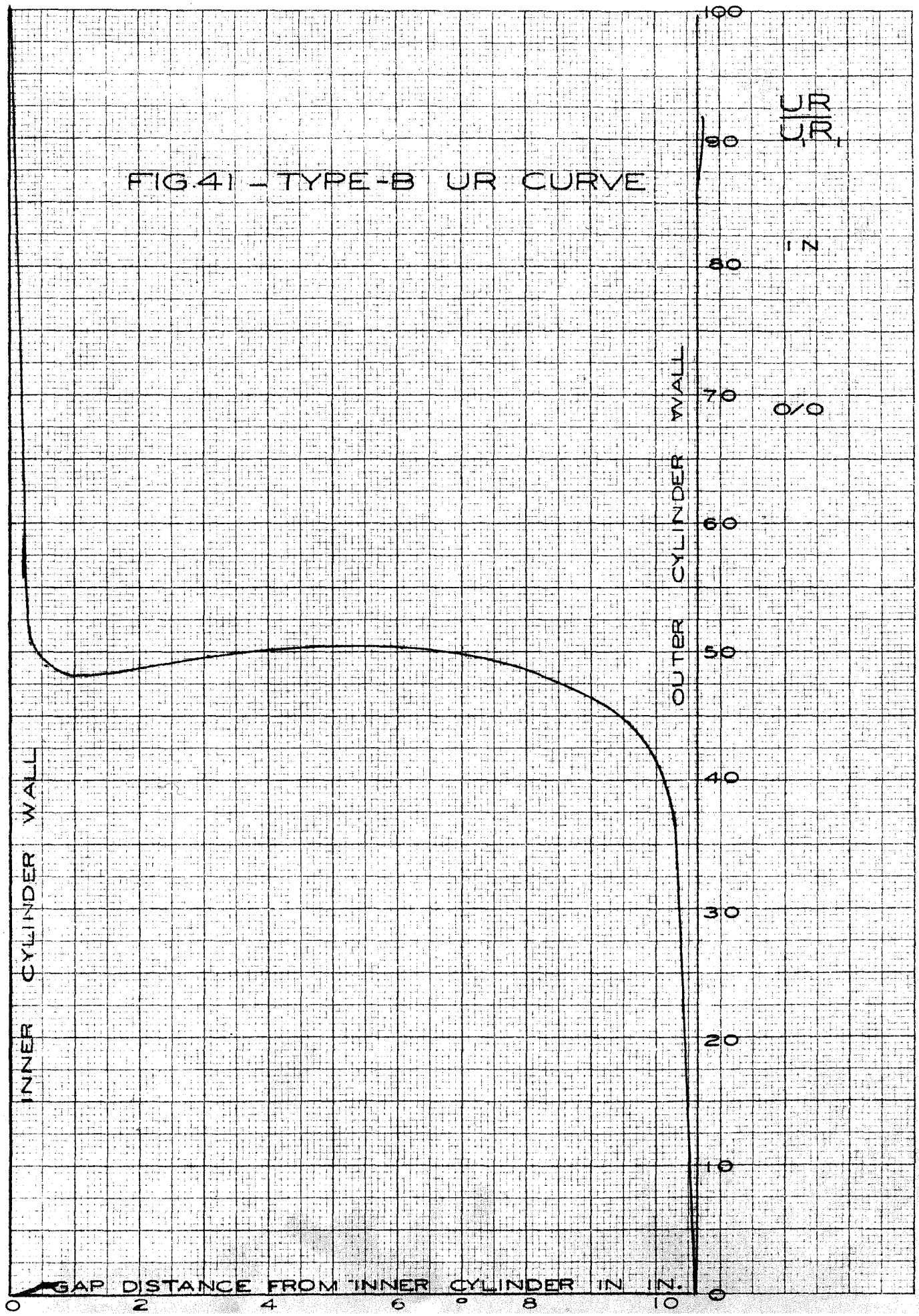
FIG.41 - TYPE-B UR CURVE
100
90
80
70
60
50
40
30
20
10
0
UR / U1R1
1 - N
0/0
OUTER CYLINDER WALL
INNER CYLINDER WALL
GAP DISTANCE FROM INNER CYLINDER IN IN.
0
2
4
6
8
10